Chapter 7 **Optical Fibre Chemical Sensing Using Direct Spectroscopy**

John P Dakin, Steven J Mackenzie and Jane Hodgkinson

1264

Chapter 7 **Optical Fibre Chemical Sensing Using Direct Spectroscopy**

John P Dakin, Steven J Mackenzie and Jane Hodgkinson

1 Introduction

It is the quantised nature of our universe, most evident at the atomic and molecular level, which allows so much information about the constituents of matter to be deduced from optical spectra. Because molecules and atoms can only emit or absorb photons (particles of light) with energies that correspond to certain allowed transitions between quantum energy states[1] optical spectroscopy is one of the most valuable tools of the analytical chemist. It can provide a rapid non-destructive analysis of many important compounds and radicals, and optical fibres permit remote on-line monitoring.

Two basic approaches are possible, either direct optical interaction with the analyte, or indirect analysis using chemical indicators; ie compounds which change their optical properties by reaction with the analyte. This chapter concentrates on the first method, that of direct spectroscopy. As stated above, the advantages are that the method is non-destructive to the sample under test and is usually very rapid. The disadvantage is that it is often not as selective as indicator chemistry, because many families of compounds exhibit similar optical properties when monitored directly.

We shall summarise the principal methods of optical spectroscopy, describe how a sensing head can be 'remoted' using optical fibre probes and discuss the advantages and disadvantages of several techniques. In chapter 10, by O. Wolfbeis, the complementary indirect methods, based on optical indicators, will be considered.

2 Basic Techniques of Optical Spectroscopy

In this section, we shall not explain the features present in any spectrum, but will simply describe how one or more features of a spectrum may be measured to determine the presence of certain chemical species. Several case studies of optical-fibre remote measurements are presented in section 3 of this chapter, but first we will present the general techniques of optical spectrometry.

2.1 Transmission Spectroscopy

Light is absorbed due to rotational and vibrational transitions of molecules, and electronic transitions of molecules and atoms[1]. The region of the electromagnetic spectrum which is efficiently transmitted (with attenuation below 10 dB/km) by silica optical fibres extends from 600 nm to 1900 nm[2]. This makes the electronic transitions and the overtones of molecular vibrational transitions accessible to remote investigation over standard optical fibres. Over much shorter lengths, near UV spectra can be measured. For IR analysis, fluoride, silver halide and chalcogenide glasses extend the (short range) possibilities to about 8000 nm, allowing the fibre-remoted study of vibrational transitions, although such fibres are both expensive and fragile.

2.1.1 Basic Concepts of Transmission Spectroscopy

This is the method most commonly used by the chemist, using an instrument called a spectrophotometer, which measures the variation of transmission of light through a sample, as a function of optical wavelength.

At each particular wavelength λ and over a small (resolution) wavelength interval $\delta\lambda$ the transmitted power, P(λ), is measured. This is given by Lambert's Law, which defines, P(λ), as:-

$$P(\lambda) = P_0(\lambda)\exp[-\alpha(\lambda)\cdot l] \quad (1)$$

where $P_0(\lambda)$ is the input power over the same wavelength interval, l is the optical pathlength through the sample and $\alpha(\lambda)$ is the attenuation coefficient at the wavelength λ. The sample characteristics are described by either:-

$$\text{a transmission factor, } T(\lambda) = \exp[-\alpha(\lambda)\cdot l] \quad (2)$$

or

$$\text{an absorbance factor, } A(\lambda) = \log_{10}\left(P_0(\lambda)/P(\lambda)\right). \quad (3)$$

For dilute solutions of absorbing compounds the attenuation coefficient, α, and the absorbance, A, are usually both proportional to the solute concentration, C. This is known as Beer's Law. The formula for the absorbance can be expressed mathematically as $A = \epsilon.c.l$, where ϵ is the (decadic) molar absorption coefficient and c is the molar concentration.

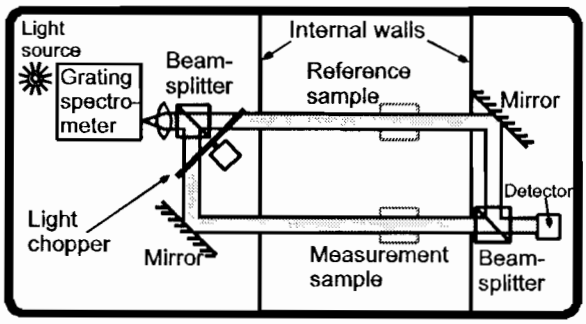

Figure 1 Schematic of Transmission Spectrophotometer

The basic principle of the spectrophotometer is shown in figure 1. A few years ago, most instruments used a grating spectrometer as a tuneable filter. In early instruments, the output beam from this was directed alternately via a sample (or measurement) channel and a separate reference channel. Most modern instruments are single channel, taking advantage of the greater stability of modern optoelectronics and computer processing. With these latter types, the measurement sequence involves a first measurement using a reference cell, storage of the transmitted signal, then measurement with the sample in the cell and finally division of the new signal by the stored reference.

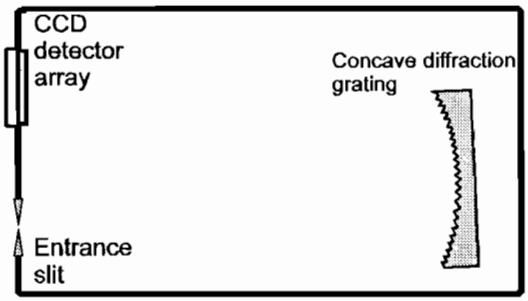

Figure 2 The latest generation of spectrophotometer, with a grating and focal plane detector.

The latest generation of instruments (figure 2), use a modified optical system, with a grating spectrometer system (with a focal plane detector array) placed after the sample. The detector array is now usually based on charged-coupled-device (CCD) technology. This arrangement effectively allows simultaneous parallel detection of transmitted signals at each wavelength. This has the attraction of greatly improving the signal/noise ratio (or reducing the signal equilibrium time). The rapid progress in CCD detector arrays suitable for the UV/ visible/ near-IR region (ie 0.2 to 1.05 μm) has led to dramatic improvement in several aspects, in particular the detection sensitivity, the number of detectors (pixels) possible and in the uniformity of response across the array. For this spectral region, the method has largely overtaken the alternative approach of Fourier Transform Spectroscopy (FTS, see section 2.8). However, when it is desired to perform ultra-high spectral resolution, or if measurements are required in the mid and near-IR region of the spectrum, (regions for which detector array technology is less advanced), FTS still has a strong position.

Working in the IR is made difficult by the presence of water, which has very strong IR absorption bands, which might interfere with measurements made. Working in the UV avoids this problem, although scattering from small particles may necessitate filtering of analytes.

2.1.2 Fibre Probes for Use With Spectrophotometers

In order to modify the spectrophotometer for optical fibre use, it is convenient to focus the light source into the outgoing fibre and couple the return fibre into the input slit of the spectrometer, but unfortunately this usually involves losses, due to the small core diameter and acceptance angle typical of optical fibre. At the remote measurement head (figure 3), it is usually necessary to collimate the light from the outgoing fibre through the sample cell (or region) and re-focus the transmitted light into the return fibre.

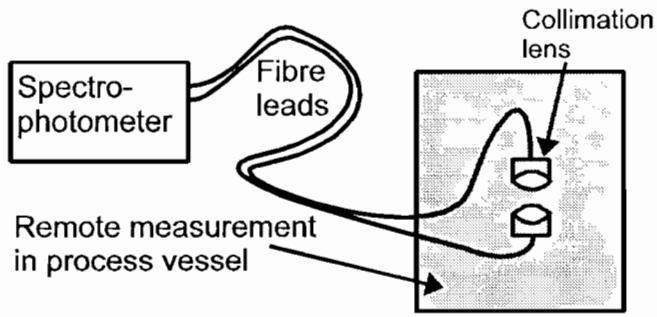

Figure 3 Remote measurement of sample absorption through optical fibres.

However, many design variations of the sensor heads are possible, for example ones having 'folded' light paths to allow the fibres to enter and leave from the top end of a 'dip-stick' type probe. For very highly absorptive samples, no optics is needed, as the measurement sample can be simply allowed to enter a narrow gap between aligned fibre ends, an arrangement that has low losses if the beam diameter of light from the fibre has not diverged to greatly exceed the core diameter of the receiving fibre.

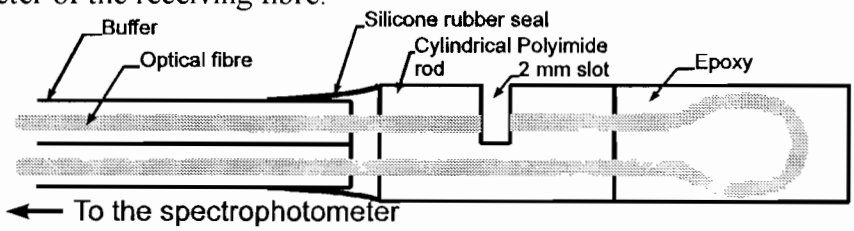

Figure 4 An early transmission probe as described by Freeman[4]

This arrangement was used in an early process control investigation, reported by Freeman in 1985[4], shown in figure 4. The ends of two fibres are separated by 2 mm and the analyte, in this case copper sulphate solution in an electroplating bath, is allowed to flow between them. The design of the probe is such that air bubbles (used to agitate the solution) do not pass between the two fibres.

Fibre optic probes can easily be used to monitor samples which have strong spectral absorption peaks, as the transmission loss in short lengths (few tens of metres) of fibre is low. The low-loss fibre transmission windows for silica-based fibres are in three main areas. The first window covers the region 700 nm to 900 nm (typical losses 3 to 5 dB/Km), the second 1050 to 1350 nm (typical losses 0.5 to 2 dB/Km) and the third 1450 to 1750 nm (typical losses 0.2 to 3 dB/Km). In low OH (dry) fibres, the first two windows effectively merge into one, as in such types the OH^- absorption at 950 nm is extremely low, whereas the peak at 1400 nm remains significant for transmission paths over 1 Km.

If the OH^- content could be kept even lower than at present, there would be a reasonably low loss window from 700 to 1750 nm. For short distance transmission (few tens of metres), however, losses for most silica fibres are moderate over the entire range from 400 nm to 2100 nm. However, if the sample has a flat, featureless absorption spectrum, or, if a quantitative measure of the absorption is required, it is necessary to provide a reference signal, in order to determine the sample properties more precisely. One method is to provide a fibre switch, to alternately direct the guided light through the sample probe and through a reference fibre path, before recombining the signals. The main technical problem is to avoid relative variations in transmission between these paths, such as may occur if there are any inter-channel variations arising from the switch, fibre-bending losses, connectors or fibre couplers.

The other problem, mentioned above, is the small acceptance aperture of the fibre. Although the small size of the fibre can be effectively enlarged using a focussing lens, this results in an effective narrowing of the acceptance angle. The effective throughput TP of a step-index fibre, as defined by the approximate relation below, remains unchanged:-

$$TP = A \cdot \pi \cdot (NA)^2 \qquad \textbf{(4)}$$

where A is the area of the fibre core and NA is the numerical aperture. At the launch end of

the system, the throughput, *TP*, represents the ratio of the power launched into fully-guided modes of the fibre, from a large area source, to the on-axis radiance of the source, when the latter is butted against the launch end of the fibre. The throughput has half the above value for graded index fibres. The throughput also determines the light intensity collected by the fibre from diffusely-scattering systems such as Raman scatterers. Clearly, large-core, high *NA* fibres are the most efficient if all the light transmitted through the fibre can be usefully employed. However, the useful numerical aperture of an optical fibre may be constrained by the acceptance *NA* of the spectrophotometer.

The total power launched into the fibres from high-radiance LEDs is rarely above a few hundred microwatts, and the spectral radiance of incandescent filament lamps is usually at least an order of magnitude less. Thus, well-designed light detection systems are required to produce practical sensors. Use of expensive high intensity arc lamps can improve matters, but laser sources are far better if ones of suitable wavelength are available.

With laser sources there is no problem in achieving launch efficiencies of over 80%, particularly into multimode fibres, and the detection-system constraints are eased substantially. Obtaining absorption spectra is much more difficult, except when using expensive tuneable types (low-cost semi-conductor lasers are however tuneable over narrow ranges).

2.2 Absorption Measurements by Attenuated Total Reflection/Evanescent Field Absorption

The technique of attenuated total reflection (ATR) spectroscopy is a commonly used tool for the study of the IR absorption spectra (from 2 to 10 μm) of, among other things, highly absorbing or turbid liquids[5]. Recently the technique has been extended through the use of optical fibres, where it is more usually referred to as evanescent field absorption (EFA) spectroscopy or evanescent wave spectroscopy (EWS)[6].

When light incident from a medium of refractive index n_1 to one of lower index n_2 is reflected at an interface by total internal reflection, some of the energy of the reflected wave penetrates the lower index medium as an evanescent field[7]. The evanescent field is not a travelling wave, and does not propagate energy away from the boundary. As the angle of incidence, α, approaches the critical angle, the penetration depth can become very large, with a proportionally larger fraction of the reflected energy present in the evanescent wave. The penetration depth also increases with increasing wavelength. If there are any absorbing components in the lower index medium, then energy is lost from the reflected wave. In this way the absorption spectra of highly opaque materials may be measured simply, without the need for ultra-thin transmission cells.

A typical bulk-optics ATR attachment (infra-red element (IRE)) for an IR spectrometer is a parallel sided glass block[5] with a partially collimated beam of light propagating in a sawtooth path down the long axis undergoing total internal reflection (TIR) at its top and bottom surfaces. When the IRE is immersed in, for example, an absorbing liquid and the light passing through the IRE analysed by a spectrometer, the resulting spectrum will contain the same information (in a slightly distorted form) as a conventional thin-cell IR transmission spectrum.

The evanescent field of a length of optical fibre (with a suitably thin cladding) may be used to perform a similar measurement. If the fibre is multimoded, then the resulting spectrum will be further distorted from the conventional transmission spectroscopy measurement due to the uneven distribution of power from each guided mode of the fibre[6]. Evanescent field sensors are particularly prone to surface contamination.

To increase the sensitivity, and remove potential masking absorptions, EFA sensors for contaminants in water often consist of polymer coated tapers. The tapered shape increases the evanescent field penetration into the polymer coating, and the latter selectively absorbs (pre-concentrates) many organic compounds, whilst excluding water. However, this renders the sensor thermally sensitive and there are delays in response due to diffusion times.

The topic of evanescent field sensors is dealt with more fully in chapter 3.

2.3 Absorption Measurement by Photoacoustic Spectroscopy

There has been much interest in photoacoustic spectroscopy (PAS) recently, and a number of textbooks have been devoted to the subject[8]-[10]. Light energy absorbed by an analyte is converted to heat, which causes the analyte and surrounding matrix (gas, liquid or solid) to expand. If the light source is pulsed or chopped, the resulting series of pressure waves may be detected using a microphone. A typical photoacoustic system is shown schematically in figure 5. Normalised absorbance detection levels (per joule of laser pulse energy) down to 10^{-9} cm^{-1} J have been measured[11].

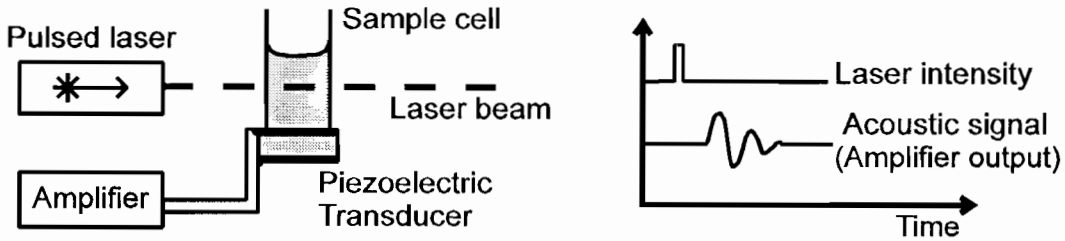

Figure 5 A typical arrangement for photoacoustic spectroscopy.

There are a number of advantages to using PAS:

i) In conventional spectrophotometry scattered light would markedly reduce the amount of light reaching the detector thus giving a spurious absorption measurement. It has less effect on the photoacoustic signal level, and so the method is less sensitive to turbidity. Light which is deflected from its path, but still absorbed, will give rise to a signal, although the effective optical path length through the sample will change by a small amount.

ii) The applicable concentration range of the technique can be large: low levels of absorption can be detected with the same equipment as high levels of absorption.

iii) The photoacoustic signal is directly proportional to the intensity of light absorbed, so there is no need to measure small differences between large light intensities, as in absorption spectroscopy. The signal/noise ratio may be much greater, and in particular the effects of source flicker noise and shot noise are greatly reduced.

The magnitude of any photoacoustic or photothermal effect will be proportional to the quantity $\beta/C_p\rho$ of the substance under analysis, where

β = volume thermal expansion coefficient of the sample
C_p = specific heat capacity of the sample (constant pressure)
ρ = density of the sample

This figure of merit is generally larger for gases and solids than for liquids. In particular, water has one of the smallest thermal expansion coefficients, vanishing to zero at 4°c, making it one of the most difficult solvents to work with.

2.4 Fluorescence (Luminescence) Spectroscopy

2.4.1 Basic Principles of Fluorescence Spectroscopy

The process of fluorescence in a compound involves the photon-induced excitation of electrons to higher energy levels (ie an absorption process), followed by their spontaneous return to a lower energy level, with consequential re-emission of a photon.

The re-emitted photon usually has a lower energy than the incident photon, as energy is often lost by phonon excitation processes (loss of energy to molecular vibrations).The lower energy emission band is called a Stokes band. A band with higher energy than the incident beam is called an anti-Stokes band.

Many aromatic compounds exhibit fluorescence when excited by UV light, but there are also some compounds and materials (eg certain organic dyes) having high fluorescence efficiency of optical re-emission when excited by less energetic photons (at other, longer wavelengths). The conversion efficiency is often expressed as a percentage, known as the quantum efficiency η, which is the percentage of the number of absorbed incident photons which result in re-emitted fluorescent photons.

$$\eta = \frac{\text{No. of fluorescent photons}}{\text{No. of absorbed photons}} \times 100\% \qquad \textbf{(5)}$$

It is essential to effectively separate the desired fluorescent light from the scattered incident light. Fortunately, this problem is assisted by the difference in wavelength arising from the inelastic nature of the fluorescence process. Therefore it is only necessary to provide effective optical filters to remove the incident light from the detected fluorescence signal. If several fluorescent compounds are present, each having different fluorescent wavelengths, they may be detected independently using wavelength-selective bandpass filters or a grating spectrometer with a focal-plane detector array. Simple forms of probe for the detection of fluorescence (or Raman scattered light) in liquids are described in section 2.7.

2.4.2 Time-Resolved Fluorescence Spectroscopy

This technique takes advantage of the statistical nature of the fluorescence processes. If a large number of molecules are excited by a short pulse of light to the same exceted state, and then begin to fall back to their ground state, then

$$I = I_0 \exp(-t/\tau) \quad \textbf{(6)}$$

where the fluorescent light intensity I decays exponentially with the time t after optical excitation. I_o is the peak intensity and τ the fluorescent lifetime.

In order to measure τ, two basic methods are used. The first (time-domain analysis) involves measuring the decay function, following short-pulse optical excitation, and computing the value of τ from this function. The second (frequency-domain analysis) uses a source with a sinusoidally-modulated incident light intensity. Either the frequency variation of the fluorescent light intensity, as the modulation frequency is varied, or the phase delay between fluorescence and excitation signals (both of which are related to the value of τ) can be monitored. Because of the weak received signal, the frequency-domain methods usually use a coherent electronic detector based on a mixer circuit. This recovers the desired frequency component in the detected signals corresponding to the original sinusoidal modulation signal. If there are compounds in the analyte having distinctly different fluorescent lifetimes, they may be separated using either of the above time-resolved techniques. Also, the time-resolved techniques are complementary to any method of separation of signals in the wavelength domain.

A more typical fluorescent process consists of the excitation of an electron, its non-radiative decay to an intermediate level and subsequent radiative transition back to the ground state. In this case the non-radiative decay is also described by an exponential decay, with its own characteristic time constant. As long as the non-radiative time constant is much shorter than the radiative time constant (as it usually is) equation 6 remains valid.

2.4.3 Limitations and Problems of Fluorescence Spectrometry

One of the primary problems of fluorescence spectroscopy is the non-linear variation with concentration at high levels of analyte, ie. when absorption of the incident light becomes large. This causes a reduction in the fluorescent signal for two reasons. Firstly, it reduces the mean optical excitation level in the sample and secondly, at high absorption levels, causes all the absorption to take place close to the point of entry of light into the sample. (In the latter case, efficiency of light collection may be less, due to geometric effects of the measurement apparatus).

Other problems can occur, due to a strong dependence of the fluorescent signals on a variety of environmental parameters. Oxygen usually quenches (ie reduces) fluorescence. The pH of a solution, its temperature and any impurities can all influence the fluorescence lifetime and intensity. In addition, many fluorescent materials can become 'bleached' during light absorption. This 'photo-bleaching' can be reversible if it is merely due to a long fluorescent lifetime (saturation behaviour), or it may, if it is due to a non-reversible photo-chemical reaction, gradually cause permanent depletion of the fluorophore. As expected, photo-bleaching is most serious at high illumination levels, but unfortunately intense sources are often used for trace analysis.

2.5 Light Scattering

There are many varieties of light-scattering photometer that can be constructed using optical fibres. However, this subject is covered in detail in Chapter 9.

2.6 Raman Spectroscopy

2.6.1 Basic Concepts

Raman scattering is observed when photons are *inelastically* scattered (ie frequency shifted) by vibrating molecules. The Raman spectra of solids, liquids or gases may be observed when a monochromatic light source (typically a laser) is used to excite the sample under investigation. Light shifted to both higher and lower frequencies can be seen, the magnitude of the shifts being equal to the characteristic vibrational frequencies of the molecule. The intensity of the light shifted to higher frequencies is, under normal circumstances, much lower than the down-shifted light.

As in fluorescence spectroscopy, photons which are inelastically scattered to lower frequencies are termed the Stokes lines in the spectrum, and those photons scattered to higher energies are anti-Stokes lines. Unlike fluorescence, any wavelength of light may be used to excite the characteristic Raman spectrum of a compound, and Raman lines are often very narrow (<20 cm^{-1}). Raman scattered light is typically several orders of magnitude weaker than fluorescent light.

The total differential scattering cross section $(d\sigma/d\Omega)_{90}$, or simply σ_{90}, is usually used to describe the Raman activity of a molecular vibration. It represents the probability of a single incident photon being scattered into a particular Raman line, in a solid angle $d\Omega$, perpendicular to the polarization vector of the incident light. It has units of cm^2·molecule^{-1}·sr^{-1}. The flux of light scattered into the collection optics of a Raman system is given by equation 7, where P_D is the incident laser power, D_a is the analyte number density, A_D is the area of the analyte under observation and Ω is the solid angle of collection.

$$\Phi = P_D (d\sigma/d\Omega)_{90} D_a A_D \Omega \qquad (7)$$

The magnitude of the scattering cross section increases very rapidly (like Rayleigh scattered light): it is proportional to the fourth power of the frequency of the scattered light. However many compounds have absorption bands in the visible and UV regions of the spectrum. If the excitation light is close to one of these bands, then the efficiency of the Raman scattering process can be enhanced by up to several orders of magnitude. However, under these conditions the Raman light may be masked by fluorescent emission, or subsequently absorbed by the material, reducing the size of the effect.

The polar distribution pattern of Raman light scattered by a molecule is similar to that of an oscillating electric dipole, ie it is zero in the direction of oscillation of the electric field vector of the incident light and is maximum at all directions in the plane at 90° to this direction. In a liquid, where all the molecules are orientated at random to one another, the radiation pattern is simply the sum of the scattering from each molecule, illustrated (for polarised light excitation) in figure 6.

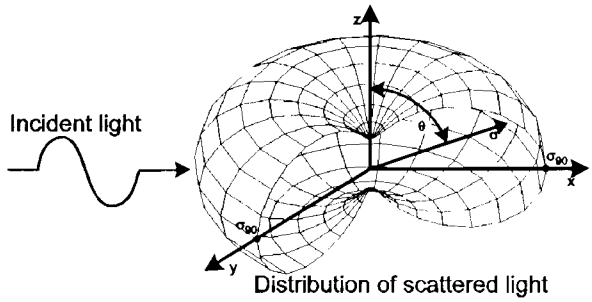

Figure 6 The average distribution of scattered light from a single molecule is the mean average of the randomly distributed scatterers throughout the scattering medium, illustrated here for the case of water.

Only those vibrations resulting in a change in the polarizability of a molecule will scatter light inelastically, and are said to be Raman active. Diatomic molecules always exhibit Raman active vibrations, and, in general, if a vibration preserves all of the symmetry elements of the molecule, then the vibration will be Raman active. Vibrations which result in particularly large changes in polarizability produce more intense Raman signals. These are often vibrations of atoms bonded by π-bonds, or large resonance bonds (eg benzene). Stronger Raman bands are normally expected from compounds of elements in the second and subsequent rows of the periodic table (as they have more electrons), from cyclical molecules (such as benzene) and hydrogenic molecules (those containing hydrogen). Liquids with large intermolecular interactions (such as those due to hydrogen bonding, in the case of water) will have broad bands, as the motion of each molecule is affected by that of its neighbours.

Typically, in a transparent homogeneous material, a proportion (of the order of 10^{-2} of the incident photons) will be scattered elastically, and a fraction of only 10^{-4} of this will be shifted in wavelength. Use of higher frequency exciting radiation increases both Rayleigh and Raman scattering. However, a compromise arises when choosing the optimum wavelength for Raman analysis, as eventually the photon energies will correspond to electronic transitions within the sample. A sufficiently high energy photon may be absorbed by a molecule (rather than scattered) and then re-emitted as fluorescence (usually after a characteristic time much greater than the 10^{-13} seconds of a Raman scattering event). Fluorescence bands are spectrally broad and can often be four to six orders of magnitude stronger than the weak Raman lines[6]. Fluorescence is not normally a problem with IR excitation, but becomes significant with incident radiation in the visible to UV region. Except for rare two-photon absorption events, fluorescence usually results in photons of a lower energy than the radiation which excites it, and so is seldom a problem in the study of anti-Stokes bands, despite the fact these are even weaker than the Stokes lines.

2.6.2 Surface Enhanced Raman Scattering (SERS)

Enhancement factors as high as 10^6 have been observed in the scattering cross sections of molecules adsorbed onto suitably prepared metal surfaces. The experimental results are remarkable, with regard to both the magnitude of the observed enhancement, and the wide range of analytes amenable to the technique. Silver, copper and gold are commonly used substrates, the most frequently used being silver. Pyridine, adsorbed on to electrochemically-roughened silver substrates displays an enhancement of up to 10^6, over a wide wavelength range extending from 500 nm to 700 nm. The enhancement factor varies for different

adsorbates, for each vibrational band of a molecule, and in addition, is a function of the excitation wavelength. Silver substrates display a maximum enhancement in the visible, between 500 nm and 700 nm[12], whereas copper and gold substrates are most efficient in the near-IR[13].

Despite its attraction for low level measurement, the use of SERS for in-situ analysis has the practical disadvantage is that it requires a carefully prepared surface, which must, by the nature of the technique, be susceptible to fouling. (One method to avoid fouling is to use a second surface layer, permeable to the analyte, eg a polymer on top of the metallic layer. However, the sensor will then be thermally sensitive and the response will be slower due to the diffusion-time delay).

2.7 Optical Fibre Probes for Raman Scattering and Fluorescence Measurements

Fluorescent light is radiated in all directions, so the coupling efficiency into the receiving optical fibres is poor at distances more than a few core diameters from the site of the emission. In addition, if the absorption coefficient is low, relatively little energy will be absorbed from the incident beam to be re-emitted. Both these aspects can be improved by using more sophisticated optical cell designs, to provide multiple passes of the incident beam through the sample and to more efficiently direct the fluorescent light into the receiving fibre.

2.7.1 Single Fibre Probes.

Only a single optical fibre is necessary to perform extrinsic measurements of wavelength-shifted, ie *inelastically* scattered light (figure 7).

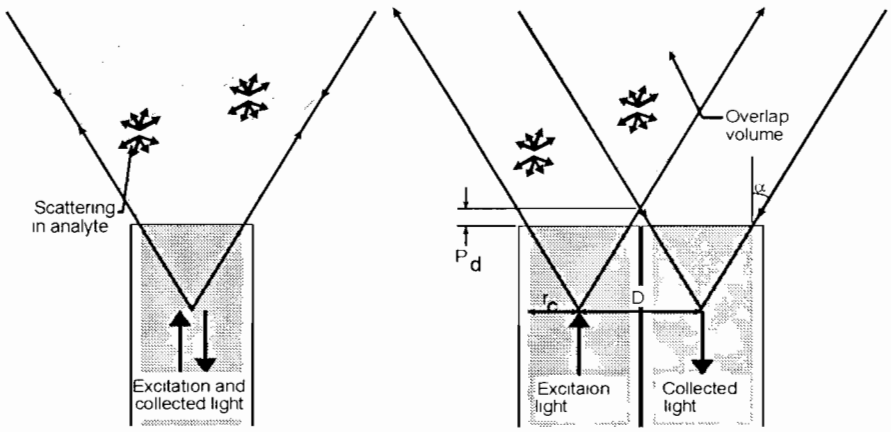

Figure 7 a) A single fibre probe; the overlap between the excitation cone and the collection cone is complete. b) A multiple fibre prove; light is only collected from part of the illuminated volume, as the excitation cone and collection cone do not completely overlap.

Probes of this type are small, cheap and efficient collectors of scattered light. They are commonly used for fibre-remoted measurements of fluorescence and absorption in the UV-VIS-NIR regions of the electromagnetic spectrum.

The sensitivity of measurements made with a single fibre probe can be limited by back reflections (Fresnel reflection) from the fibre tip. Polishing the tip of the fibre at an angle can eliminate back-reflections from the probe tip, but distributed backscatter from the whole

length of the fibre is unavoidable. Although a spectrometer with suitably high stray light rejection may be able to remove scattered and reflected light at the incident wavelength, Raman scattered light and fluorescent light originating within the fibre core will interfere with weak signals from the analyte when a single fibre probe is used.

The unwanted fibre fluorescence, which is normally particularly troublesome with UV or short- wavelength visible excitation, is less intense when using high OH^- content (wet) silica, UV-grade, fibre. Generation of Raman light within the silica cannot be similarly avoided as this broadband scattering results from the vibrations in the glass itself, although these vibrations are all below 1400 cm^{-1}. A measured Raman spectrum of pure silica glass is shown in figure 9. These interfering components can be almost entirely rejected from measurements made through multiple optical fibre probes[14].

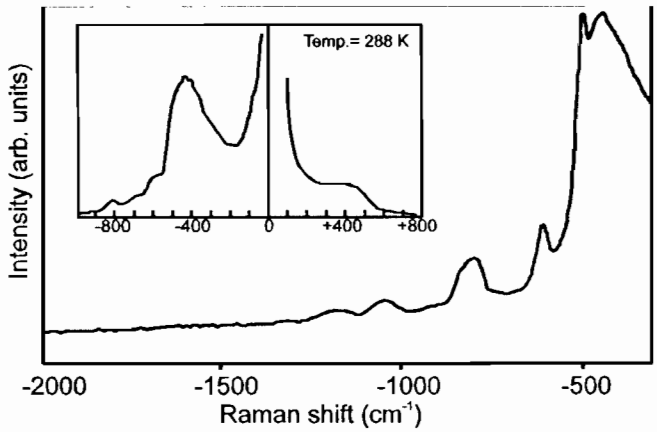

Figure 8 The (Stokes) Raman spectrum of a fused silica fiber, recorded by Ma[15], with the low wavenumber and highly temperature dependant anti-stokes spectrum shown inset.

2.7.2 Multiple Fibre Probes.

By using separate optical fibres to carry light to and from the probe the optimum placement of optical filters can be used to reject any potentially interfering light. A narrow band pass filter after the delivery fibres ensures only light at the excitation wavelength reaches the sample, and is essential for probes to be used in Raman measurements. A notch filter (or a long or short pass filter) before the collection fibres removes any unshifted light which could generate fibre Raman or fluorescence between sample and spectrometer. In fact, much more unshifted light than shifted is usually collected in a Raman measurement, so removing this component can dramatically reduce the stray light within the spectrometer too.

The designs of the probes themselves fall into two broad categories: Those where separate delivery and collection fibres are used in the probe, and those where the light from the delivery and collection fibres is multiplexed into a (short) length of a single fibre. Probes in the first category are relatively inefficient, due to the incomplete overlap of their emission and collection cones. In fact no light at all is collected from points closer than P_d (see figure 7). The distance P_d is linearly related to the separation between the fibre cores, D:

$$P_d = \frac{2 \cdot r_c - D}{2 \cdot \tan(\alpha)} \qquad \textbf{(8)}$$

where r_c is the core radius of the fibres and α is the collection half cone angle. It has been proposed that probes formed of concentric rings of collection fibres around a central delivery fibre (a fairly common arrangement) could be used to perform depth profiling measurements[16]. While this idea is sound in principle, it is hard to think of possible practical applications.

An example of the second category of probe is shown in figure 9. Light is coupled in and out of the short sensor stub via a colour separation filter, which can efficiently reflect light in one band of wavelengths while transmitting light outside that band. The excitation and collection cones then overlap as in a simple single fibre probe, with a similar high collection efficiency. Unfortunately filter transmission is typically below 80%, or lower if a sharp transition between transmitting and blocking (or reflecting) regions is required.

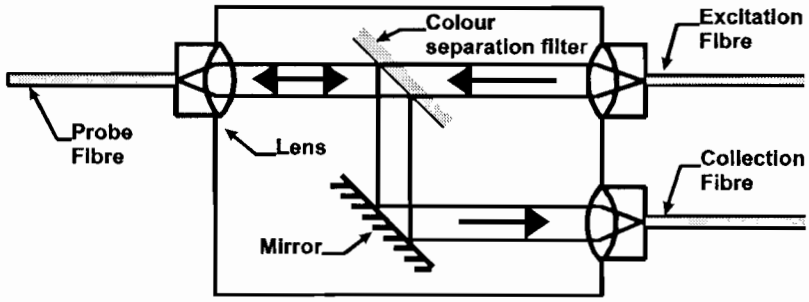

Figure 9 Use of a colour separation filter allows excitation and collected light to be combined in a short length of fibre at the probe tip. Short wavelength light is transmitted by the colour separation filter, whereas longer wavelength Raman scattered light is reflected

2.7.3 Improving the Efficiency of Optical Fibre Probes

An immediate advantage of using bundles of optical fibres to collect light scattered from an analyte is that a circular light-collection area is easily transformed to a linear slit at the spectrograph input. Light is usually most efficiently collected from a circular region of the analyte (for instance around a focused spot of excitation light). The resolution of a dispersive spectrometer (ie one in which the different wavelengths of light are separated by a diffraction grating or prism) is usually limited by the width of the input slit. By rearranging the collection fibres to be a linear array at the spectrometer input, the maximum possible throughput is achieved at a given resolution.

The amount of light collected by multiple fibre probes may be increased either by arranging the collection fibres at an angle to the excitation fibre, or by angle-polishing the tips of the emission and collection fibres with respect to one another (figure 10). An angle of 9° between 0.22 NA fibres will increase the collected light intensity by about 70% with respect to parallel fibres in a clear colourless analyte. The optimum angle increases as the fibre NA increases[17].

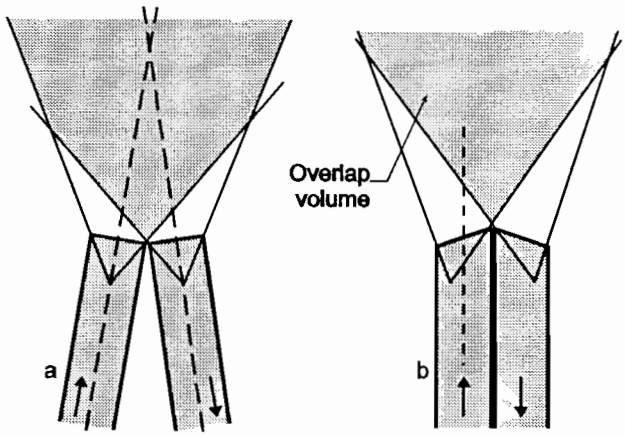

Figure 10 The overlap between the emission and collection cones may be increased by a) angling the two fibres with respect to one another b) angle polishing the tips of the fibres.

The amount of light collected by an optical fibre bundle can be increased by using a lens to focus the excitation light to a spot in the analyte, and the scattered light back onto the bundle. This may be economically achieved using a sapphire ball lens. Use of lenses also facilitates non-contact measurements.

For liquid analytes, light may be confined within the numerical aperture of the probe fibres over even longer distances by enclosing the analyte in a reflective tube of diameter approximately equal to the diameter of the fibre probe. In this way, a long measurement length may be used, whilst maintaining a confined beam (with consequent increase in collected signal intensity). Although the sampling length is increased, the actual volume is very low when using small diameter tubes.

2.7.4 Commercially Available Optical Fibre Probes

Convenient and rugged examples of all the probe arrangements described above are available commercially. Polytec manufacture a range of probes for optical-fibre-remoted measurements of absorption (both transmission and ATR), reflectance and scattering, mainly intended for use with their X-dap diode array spectrograph[18]. They also sell a fibre coupled cuvette holder and a flow through cell.

Dilor manufacture probes such as the Dilor Super-Head distributed through Instruments SA, illustrated in figure 9. This is marketed specifically as a probe for Raman spectroscopy, and may be arranged to multiplex measurements at several different points. Hellma manufacture immersion probes for transmission measurements, designed to work with any standard photometer. The Savannah River Technology Company manufacture a probe with angle polished tips for increased collection efficiency and micro-filters at the probe tips. This probe has been used for diffuse reflectance, fluorescence and Raman measurements[19].

Probes which can be interfaced via a standard cuvette holder are available as add-ons, eg from Hellma, for any transmission spectrophotometer[20]. The probes can be made rugged and chemically resistant, and due to the optical nature of the measurements, the method is intrinsically safe in flammable areas and immune from electromagnetic interference. Efficient probes for collecting fluorescent or Raman light are available from FCI[21],[22]

2.8 Fourier Transform Spectroscopy

This is not so much a spectroscopic arrangement, rather a generic means of processing the optical signals without the traditional monochromator to analyse the light spectrum. The method involves detection of the optical signal, via an interferometer having a scanned path-length difference. A two-path interferometer acts as an optical filter, having a periodic transmission T(v), with a function of optical frequency v where:-

$$T(v) = 1 + \sin(k(v)) \qquad \textbf{(9)}$$

The constant, k, depends on the optical path differences in the interferometer. The detected signal $S(v)$ when a complex light spectrum $I(v)$ is, after passage through the interferometer, incident on a detector with a spectral response $D(v)$. $S(v)$ is given by:-

$$S(v) = \int_{v=v_{max}}^{v=v_{min}} I(v) \cdot T(v) \cdot D(v) \, dv \qquad \textbf{(10)}$$

The function S represents the correlation between the sinusoidal transmission function of the interferometer and the combined spectral responses of the input light spectrum and the spectral response of the detector. Clearly, the correlation is best with spectral variations having the same (optical-frequency) periodicity as the interferometer. In the simplest case, where $I(v)$ is a narrow line spectrum of constant frequency, the signal S represents a single (sample) point on the sinusoidal response. If the pathlength of the interferometer is now scanned, its periodic transmission-response function will translate across the frequency band (and also change its period versus frequency). The detected signal will therefore vary, as the correlation between the spectral features and the periodic interferometer response varies. In the simplest case of the line spectrum, the detected signal will vary sinusoidally as the interferometer is swept. More complex spectra can be considered to consist of a linear addition of a series of such narrow-line spectra, each having an appropriate amplitude. For a complex spectral response, the variation of the detected signal with time, as the interferometer is swept, represents the inverse Fourier transform of the original spectrum. The spectrum can therefore be recovered by Fourier transformation of the temporal variations in detected signal, resulting when the interferometer is scanned. This is again illustrated by the simple example of the line spectrum, which results in a sinusoidal temporal response. The Fourier transform of a sinusoidal signal has a single value, corresponding to the single frequency of the line spectrum.

When compared to conventional spectrometers, the Fourier transform system has several advantages. The first is that it is relatively easy to obtain high spectral resolution by using a long 'path' difference interferometer (10 cm path difference at 1 μm wavelength, results in a fractional resolution of around 1 part in 10,000). The second is that a significant fraction of the source light is incident on the detector at all times, because the mean transmission of the interferometer is much higher than that of a narrow band grating monochromator, thereby improving the optical efficiency. The third is that the interferometer can be designed with a large optical aperture, giving much higher optical throughput from radiance-limited optical

sources. The advantages are less significant when only moderate resolution is needed and low-noise (eg CCD) detector arrays can be used, as these also allow parallel detection of each spectral component.

The main disadvantage is normally the need for a precisely-aligned interferometer, with its necessary thermal and mechanical stability. Fourier Transform spectroscopy is applicable to a wide variety of spectroscopic techniques, including transmission, reflectance, fluorescence and Raman spectroscopy, as, in all of these cases, it can be used for spectral analysis before the detection system.

2.8.1 All-Fibre Fourier Transform Spectrometer

This ingenious method[23] involves interference between unequal-length, guided-wave light paths in monomode optical fibre. Light from a broadband source is passed through an absorbing medium, and then a variable-path, all-fibre Michelson interferometer. To produce the spectrum of the transmitted light, the Fourier transform is taken of the time-varying detected signal as the path difference is mechanically-scanned. The fibre Michelson interferometer has one piezoelectrically-stretched fibre arm and one unstretched arm. The system has yet to be tried for low contrast applications, such as optical gas detection, but has been successfully used to measure the spectrum of a semiconductor laser source, at various levels of injection current. For applications such as gas detection, the usual signal/noise advantage when operating at high resolution in the Fourier transform domain should, however, be achievable. The restriction arising from single mode operation will, unfortunately, cause a severe loss of light compared with the multi-mode approach generally used in gas sensing systems.

One feature of the fibre-based FT spectrometer, not associated with normal types is that the optical delay will be wavelength dependent due to fibre dispersion.

3 Case Studies of Fibre Optic Sensors Using Direct Spectroscopy

In this section, we shall describe a number of areas where fiber optics has been used for direct spectroscopy.

3.1 Liquid Phase Sensing

Many liquid sensing applications may be carried out using extension leads from a commercial spectrophotometer. Some manufacturers now sell such attachments as optional extras for their commercial instruments. High-concentration solutions often exhibit strong absorption spectra, so there is seldom a need to develop the specialist instrumentation of the type required for low-contrast gas detection (see the next section). The measured spectra can be used for the simultaneous determination of several absorbing solutes by using multi-variate analysis methods[24],[25]. These are essentially computerised methods, capable of adding the various spectral features characteristic of each *expected* analyte, in appropriate proportions and finding the best match to the experimentally observed spectrum. Clearly multi-variate analysis becomes difficult, if not impossible, if several analytes with very similar absorption spectra are present. The problem becomes insoluble if unexpected contaminants with strong unknown spectral characteristics are present.

Better results are claimed in these circumstances for techniques incorporating artificial neural networks[26],[27] which are easily implemented as computer software. Neural networks can be fast and tolerant of imperfect data, but care must be taken to use them within their limitations[28]: The network must be optimally 'trained' by presenting it with a suitable number of reference spectra which should encompass data in every form in which it might be subsequently encountered (eg, buried in noise or in the presence of contaminants).

In addition to simply measuring the transmission of a collimated beam of light through a sample, there are a number of other ways in which the qualitative absorption spectrum can be deduced. Indeed, the first recorded demonstration of an optical fibre absorption measurement (by M Polani in 1962)[29], used 50 μm core glass fibres to measure the diffuse reflectance of blood at 805 nm and 660 nm. From these measurements, the absorption spectrum of the blood around 660 nm, and hence its oxygen saturation could be determined. By using the non absorbed wavelength of 805 nm as a reference fluctuations in parameters such as fibre bending losses could be corrected for. The small size of optical fibre probe heads (and chemical resistance of silica components) mean that very little interference is caused to any process under observation.

Many recent applications of spectroscopy to industrial process control (many using optical fibres) are presented in recent SPIE volumes, eg *Optically Based Methods for Process Analysis*[30] and *Optical Sensing for Environmental and Process Monitoring*[31], and in journals such as *Process Control and Quality*. We shall now examine examples of spectroscopic methods in more detail.

3.1.1 Transmission Spectroscopy

This technique has found wide application in chemical, biological and environmental monitoring and process control, due to its generic nature, intrinsic safety and ease of application. In 1988 Boisde reported that over a kilometre of optical fibre had been installed at French Atomic Energy Commission sites for the purpose of on-line process monitoring[32]. The samples monitored ranged from measurements of a single species in a restricted analytical medium, through simultaneous determination of several species, (possibly with mutual interference) to trace measurements in a complex medium. In some cases, single wavelength measurements were appropriate; in others full spectral measurements were necessary. It was claimed that the first (unpublished) work was done as early as 1974, with differential measurement at wavelengths of 477 nm (absorption peak) and 520 nm (low absorption reference wavelength) monitoring Pu (IV) concentration in aqueous solution.

The simple fibre-fibre probe of Freeman[4], which was described in section 2.1.2, was used to determine copper sulphate concentration in an electroplating bath. Light from a 820 nm LED was coupled into one of the fibres, and a fraction of the light transmitted across the gap was collected by the other fibre. The intensity of this light was then measured by a photomultiplier (although a photodiode could probably have been used). Freeman found excellent correlation between the Cu^{2+} concentration and the absorbance of the light transmitted between the fibres over the concentration range 0.2-0.4 M.

Of the other constituents of the plating bath, sulphuric acid was found to influence the transmission the most, with increased sulphuric acid concentration lowering the apparent

absorbance of the solution.

For a simple fibre-fibre probe, changes in the refractive index of the analyte can modify the output-light cone angle to a different extent at the reference wavelength than at the measurement wavelength (optical dispersion). This problem can be reduced by lensing the fibres, so that the light is collimated before it enters the sample. Researchers at the Westinghouse Savannah River Company (Aiken, USA) have been developing absorbance probes for in line monitoring since the 1970s[21]. A lens assembly from one of their probes is shown in figure 11.

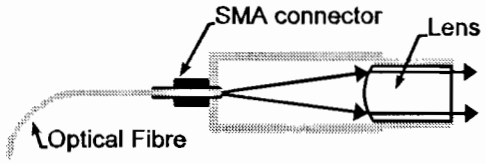

Figure 11 Savannah probe lens assembly[21].

These probes have been used in pairs, for instance across a process stream, with light transmitted through the analyte from one assembly to another. Because the light is collimated when it leaves the flat glass-liquid interface, changes in the refractive index of the analyte have less effect on the intensity of collected light.

An alternative arrangement is to position a mirror facing the end of a single optical fibre. A medical application of a single fibre probe using a fixed mirror is described by Coleman, who used an optical fibre threaded through a hyper dermic needle with an aluminium reflector close to its tip[33] shown in figure 12. Coleman described applications for in vivo analysis in regions previously too small to sample, and presented in vitro measurements of bilirubin in human blood. By using a 25 mW argon ion laser source at 457.8 nm, Coleman measured a minimum detectable absorbance of 0.005 m^{-1} corresponding to bilirubin concentrations between 0.05 M and 1.3 M.

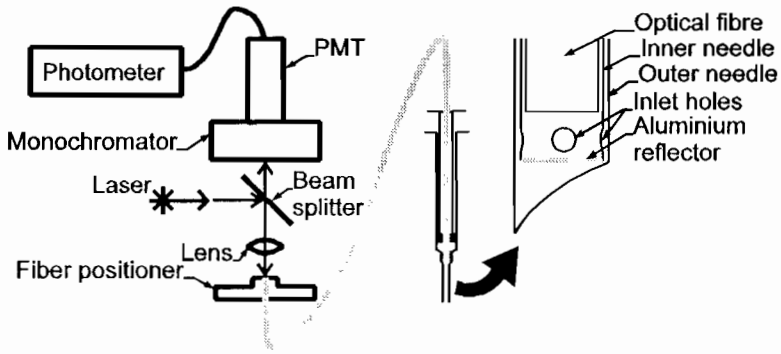

Figure 12 In vivo arrangement described by Coleman[33]. The optical path length is twice the distance between the fibre tip and the reflector.

3.1.2 Evanescent Wave Spectroscopy (EWS)

This topic is covered extensively in chapter 3 of this volume, but we shall briefly discuss a few applications here. The arrangement is similar in each case: light is transmitted through a

section of optical fibre, either unclad or with a very thin cladding, which is immersed in to the analyte. As mentioned earlier, a polymer buffer layer is often applied to the fibre in the sensing region. This can serve the dual purpose of excluding solvent from the evanescent wave region, and pre-concentration of the sensed species: a hydrophobic species may dissolve in very low concentrations in water, but will preferentially move into a polymer layer. Sensitivity is increased by using longer and smaller diameter sensing fibres, and is also enhanced by coiling the fibre with a small bend radius.

Mid-IR fibres have been used for EWS, but only as short detection elements, limiting the range of remote measurements to a few tens of metres from the interrogation system[34]-[37]. Krska has used 10 cm lengths of silver halide fibres, coated with low density polyethylene (LDPE), to detect 50 mg/l of trichloroethylene in water, using a black body source and FTIR spectrometer. By using a 0.5 mW lead-salt laser diode, temperature tuned over the range 847 cm^{-1} to 1099 cm^{-1} (approximately 12 to 9 μm), and coupled to a simple photodiode detector, a concentration of 0.1 mg/l could be detected, in a measurement time of 55 seconds (albeit after allowing a 10 minute interval for enrichment by diffusion into the polymer).

Degrendpre and Burgess have used 1.5 m of 400 μm core polysiloxane clad fibre, coiled on a 3 cm diameter Teflon support[38], to study the absorption (in the range 1-2.2 μm), of neat organic solvents, and mixtures of chloroform in carbon tetrachloride and of carbon tetrachloride in toluene . Bürck has reported detection limits of between 80 mg/l (dichloromethane) and 0.1 mg/l (1,2,4-trichlorobenzene) for various chlorinated hydrocarbons. Using a 10.58 m long, 400 μm core, sensing fibre, clad with polysiloxane,[39] the 90% response (diffusion) times ranged from 0.5 min for dichloromethane and 71 minutes for 1,2,4-trichlorobenzene[40]. Initial experiments by Schwotzer with polysiloxane or Teflon-AF (5-20 μm thickness) coated fibre of 140 μm core diameter have shown detection limits of 10 mg/l for toluene and 0.05 mg/l for napthalene (both in water)[41]. These results were obtained using 0.5 m of fibre coiled with a diameter of 1 cm.

3.1.3 Photoacoustic Spectroscopy

As previously mentioned, a photoacoustic signal results from the absorption of radiation, followed by dynamic pressure changes due to thermal expansion. The following case studies illustrate the variety of methods used to detect a photoacoustic response. The technique is applicable to gas or liquid phase sensing (although the detection schemes may vary), and the examples in section 3.2.6 of this chapter may also be of interest.

Detection of photoacoustic surface movement

In condensed phase samples, a bulk pressure wave may cause the displacement of a free surface, which can be sensitively detected in a number of optical ways[42]. These include measurement of the curvature, gradient, or displacement of the surface.

Hand et al have used a fibre-optic Michelson interferometer to measure the displacement of the surface of liquids[43],[44]. A pulsed Nd:YAG laser was used as the pump source, directed onto one focus of an elliptical cell. Acoustic waves generated in this region were reflected by the cell walls to form a second focus at the liquid surface of the cell, thus amplifying the displacement. The resulting transient surface deflection was detected with the interferometer.

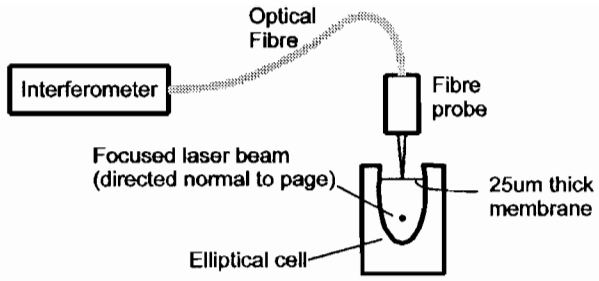

Figure 13. Apparatus used to detect surface movement caused by photoacoustic waves in an elliptical cell (modified from Hand[43]).

Two different types of cell were used; the first with an open liquid surface at the top of the cell, and the second using a thin, more-highly-reflective membrane in contact with the liquid surface. Using the latter method, figure 13, the interferometer had a noise floor of $2x10^{-14}$ m.Hz$^{-½}$, and a pressure sensitivity of 0.1 Pa.Hz$^{-½}$ was demonstrated.

Using pulsed optical excitation offers a number of advantages, at the expense of an increase in system cost and complexity :-.

- The acoustic pulses produced have a large high-frequency component, enabling the short-wavelength pressure waves to be focused by a small cell (giving a fourfold signal enhancement, as reported by the authors).
- Time gating the transient response removes any spurious signals arising from absorption at the cell windows, which can otherwise be a significant limiting factor in photoacoustic spectroscopy[45].

Detection of photothermal refractive index changes

A photoacoustic volume change may cause a corresponding change in the refractive index of the sample medium, which can be detected using thermal lensing techniques, photothermal deflection, or measurement of the optical path length through a sample.

Thermal lensing and photothermal deflection spectroscopy (PDS) have been comprehensively reviewed by Tam[46], and are particularly suited to the analysis of liquid phase samples. Thermal lensing occurs when a beam of light (usually from a laser) is partially absorbed by an analyte, to cause a thermal gradient in the fluid. The resulting refractive index changes create a transient lens in the sample, which usually defocuses the beam. This may be detected using a photo-detector having a small acceptance aperture.

In photothermal deflection spectroscopy, higher sensitivity can be gained using a second CW beam, not absorbed by the analyte, to probe the refractive index changes. A detector may be split into two halves, such that a deflected beam has an increased intensity on one half and a decreased intensity on the other. The ratio of the two intensities gives a measurement which is unaffected by changes in the source intensity. Different possible configurations are;

so-called 'collinear PDS'
- Probe beam at a small angle to the pump beam, to give a large interaction length.
- Probe beam parallel with the pump beam, but displaced to the point of maximum response (maximum $\partial n/\partial r$).

'transverse PDS' - Probe beam orthogonal to the pump beam.

Bohnert and co-workers have used both collinear and transverse PDS for the trace detection of pesticides in water[47]. A schematic diagram of the apparatus used for transverse operation is shown in figure 14.

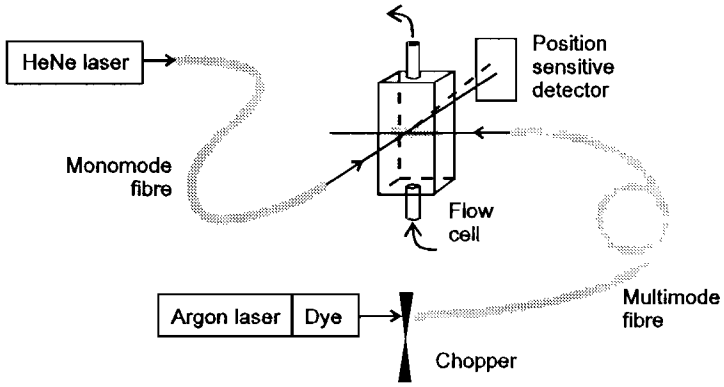

Figure 14. Schematic diagram of sample cell used for transverse photothermal spectroscopy of pesticides in water. Picture modified from Bohnert[47].

Transverse PDS was compared with a state-of-the art spectrophotometer (Cary 2400), which had a low noise level corresponding to an absorbance of 0.0002 AU. Detection limits for a number of pesticides were better for the photothermal method, by factors ranging between 2 and 20 for various compounds. Collinear PDS improved the detection limits by a factor of four, so that for example, 2,4-dinitrophenol would be detected at the 0.5 ppb level. The fact that different pesticides responded differently might be explained by differing photoacoustic generation efficiencies for each chemical. Clearly, a strong photoacoustic signal is only possible if the energy absorbed by a molecule is converted to heat rapidly, ie within the integration time of the experiment. Other non-thermal relaxation pathways are possible for molecules, including fluorescence.

Refractive index changes have been observed in the liquid phase by Vegetti et al[48], who placed their sample (water containing trace quantities of a dye) in one arm of an optical interferometer, and detected the resulting phase change in the probe beam (see figure 19). They employed an argon ion laser (modulated at 4 kHz), as their excitation source, arranged to be close and parallel to one arm of a Michelson interferometer. With this equipment, detection of phase differences as small as 5×10^{-7} rad was demonstrated, corresponding to a detection limit of 1.5×10^{-4} absorbance units for a 1 cm pathlength.

3.1.4 Fluorescence Spectroscopy

Remote monitoring of sample fluorescence via optical fibres is a long standing in-situ monitoring technique. Measurements made by fibre probes can provide qualitative and quantitative information, with an additional degree of selectivity provided by the choice of excitation wavelength and the fluorescent lifetime of a particular analyte. Although broad band sources can be used to excite fluorescence, lasers are usually preferred for use with optical fibres, as their output is more easily focused to a small spot. The acronym LIF is often used for laser induced fluorescence.

Ground water monitoring of Uranium was carried out by workers at the Lawrence Berkeley and Lawrence Livermore laboratories in the US[49]. Their attractive method of uranium detection was based on its fluorescence, when excited at 488 nm by an argon ion laser source. There are strong fluorescence lines at 520 nm, 527 nm and 530 nm and the technique has now been used in the laboratory down to levels of 10^{-14} molar.

Because fluorescence bands are quite broad, the additional information provided by fluorescent lifetime measurements is often necessary to distinguish compounds. For instance, Chudyk found that phenol, toluene and xylene (all single-ring aromatic compounds, with peak emission around 295 nm) were initially indistinguishable in their vapour phase[50]. However, by measuring the fluorescent decay time τ with a pulsed 266 nm source, phenol (τ = 2.1 ns in cyclohexane[51]) could be easily distinguished from toluene (τ = 34 ns) and xylene (τ = 31 ns).

The electronics required to perform time-resolved fluorescence spectroscopy (TRFS) has been simplified by Bublitz[52]. By counting photons from the fluorescence in two adjacent arrival-time windows and ratioing the counts, engine oil in water was detected at concentrations below 1 mg/l, and polyaromatic hydrocarbons (PAH) concentration at the µg/l level. The fluorescence was excited by a 2 ns pulse from a multi-gas UV excimer laser, using 248 nm to excite the BTEX compounds (benzene, toluene, ethylbenzene and xylene) and 337 nm for PAHs. Light was emitted between 260 nm and 370 nm for BTEX and between 370 nm and 500 nm for PAHs. The initial laser pulse triggered two gated photon counters, first from 0 to 100 ns, and then from 120 ns to 220 ns after the initial laser pulse.

The light emission from impurities in natural water had a short decay time, and the photons from this source were counted in the first time window. The signal count in the second window was thus due to the longer-decay-time contaminants. By taking the ratio of the two signals the concentration of impurities could be deduced from a look-up table. The PAH emission wavelength coincided with the emission of the natural humic matter, and a further parameter had to be introduced to account for this.

Better detection limits for detecting PAHs in situ[53] were achieved by Panne and Neissner. Full TRFS was used, and detection limits down to the ng/l range were achieved for benzo-fluoranthenes and benzo-pyrenes. The probe consisted simply of two 600 µm core diameter silica fibres, angled at 11° to each other, with their end faces close together. The collected light was transmitted to the input of an f/3.8 spectrometer via a circular-to-linear fibre-bundle converter (for increased resolution), and a photodiode array at the focal plane was used to resolve the wavelength spectrum. The laser was pulsed (0.6 ns FWHM) and the detected signal was gated, to integrate for 5 ns at any time after the pulse. After deconvolution of the system response, a time resolution of 0.5 ns was claimed.

One problem encountered with high optical power at wavelengths below 350 nm is photo-degradation of the optical fibre. Interaction of intense UV light with silica fibres leads to fluorescence and a decrease of fibre transmission through the formation of colour centres. Although this damage is minimised by using so-called 'UV-enhanced', high OH^- fibre, Hillrichs proposed placing a frequency doubling arrangement at the *probe* end of the transmission fibres[54]. The excitation light is then efficiently transmitted through the fibre at 532 nm, with a relatively low attenuation coefficient (0.16×10^{-4} cm^{-1}, compared with

11.5×10^{-4} cm^{-1} at 266 nm) and without significant photo-degradation of the fibre. Despite the fact that the energy is converted (in a small BBO nonlinear optical crystal[55]) to 266 nm with only 1% efficiency, Hillrichs calculated that, for fibre lengths over 30 m, this is the most efficient way to transmit light to the sample, and, in any case, avoids cumulative damage to the fibre.

3.1.5 Raman Spectroscopy

Fibre remote Raman spectroscopy has found many applications in a wide range of process control and remote monitoring applications. The interest in the technique stems from its generality and its compatibility with cheaply available optical fibre components. Approximately as wide a group of compounds as for IR are amenable to the technique, and qualitative and quantitative information can be deduced from the Raman spectrum without any need for indicator chemistry. Any wavelength of light may be Raman scattered by a molecule, and the optimum for many analyses lies conveniently within the transmission window of silica optical fibres, which efficiently transmit visible and near-IR light (but not the wavelengths used in most IR absorption work). The major weakness of the technique is the low intensity (generally four to six orders of magnitude lower than typical fluorescence) of Raman scattered light, and much work has been done to efficiently collect this light and separate it from any interference.

A common problem in measuring Raman spectra of (in particular) organic molecules is sample fluorescence. By using time resolved methods as described in section 2.4.2 longer lived fluorescence can be eliminated from (effectively instantaneous) Raman scattering by pulsing the excitation light source and gating the detector so that only 'early' Raman light is received. For samples containing only one fluorescent component, Raman light can be separated by phase resolved methods, such as that demonstrated by Demas[56].

Demas demonstrated the nulling of unwanted fluorescence signals from Raman spectra by modulating the excitation light. The fluorescence lifetime of a fluorescent compound is usually significantly greater than that for the Raman scattering process, so the frequency of modulation can be varied until the fluorescence signal is 90° out of phase with the Raman signal. Lock-in detection can then be used to reject the fluorescent light. Demas resolved the Raman spectrum of water from a solution of rhodamine 6G laser dye (excited at 514.5 nm). Although results were good, the phase resolved technique is essentially analogue, and so it is most suitable for use with scanning monochromators (rather than spectrographs using multi element output arrays), which makes for long measurement times. A time constant of one second was used to resolve Raman peaks barely visible in the non-phase resolved measurement, much more successfully than by subtraction of a normalised background measurement of rhodamine fluorescence. Demas postulated that slight errors in the systems cancellation of the fluorescent background may be due to variations of the fluorescent lifetime of two overlapping bands of the single fluorescent molecule, limiting the techniques ultimate sensitivity.

An obvious means of maximising the amount of Raman scattered light generated within a sample is to pass the excitation beam through the cell multiple times, or to use an arrangement in which the excitation light has a large interaction length with the sample and subsequently scattered light is guided to the collection optics, such as a capillary cell. If the

walls of the capillary are sufficiently thin light launched coaxially travels mostly within the analyte. Even better, if the walls of the capillary are made of a material with a lower refractive index than that of the analyte, a waveguide is formed which confines the excitation and scattered light emitted within the collection optics of the spectrograph to the capillary. Walrafen reported enhancements of up to 1000 times by using such capillaries of up to 25 m in length for the Raman spectrum of benzene. Unfortunately large numbers of potential analytes have refractive indices lower than that of silica (1.47), eg most aqueous solutions. The fabrication of capillaries with a refractive index lower than water (1.33) is very difficult, however new results using members of the Teflon-AF family of fluoropolymers ($n<1.32$) have demonstrated water cored wave guides with potential for wide application for analysis of water based analytes[57].

The cure process of epoxy resins has been studied using Raman spectroscopy via optical fibre, for instance by Chike[58]. Fully utilising the information available in the Raman scattered light from the material both the extent of the cure process, and the temperature of the system were measured. The temperature could be measured by comparing the intensity of the anti-Stokes Raman shifted light (light shifted to a shorter wavelength), which changes exponentially with temperature. The variation of the Stokes lines is only slight and hence the ratio of the two measurements can be used to deduce the temperature at the sampling point. The degree of cure was calculated by taking the ratio of the epoxide ring stretch at 1240 cm^{-1} which is linearly dependant on the progress of the cure and the 1186 cm^{-1} vibration of a component not affected by the cure. These results were compared with infra-red absorbance measurements (through 1 mm of sample), and found to be in excellent agreement, and although the infra-red measurements were made at close to optimal conditions, the authors felt that there was room to improve the apparatus for the in-situ Raman measurement.

The arrangement used to gather the Raman light from within the epoxy composite was simply a pair of parallel 200 µm core optical fibres bonded into an SMA connector, and polished down to 3 µm finish. This 'pencil probe' arrangement was simply dipped into liquid samples prepared with a suitable epoxide concentrations to simulate the glue at various stages of cure. In practical applications such parallel fibres could be left within the material after cure, possibly for use as sensors for chemical degradation or to measure the temperature of the material in use.

An application in the nuclear industry for which the technique has been investigated is the detection of water in sodium nitrate slurry[59]. Although Raman is not the most obvious technique for this application (water has very strong IR absorption bands and would be easily identified by these) the Raman information would be obtained as a bye-product of other measurements made. Two approaches were investigated, first the direct detection of the water bending vibration around 1630 cm^{-1}, and more successfully by taking the ratio of the intensities of the solid sodium nitrate Raman line and the intensity of the dissolved nitrate line (which is shifted by 17 cm^{-1}).

Direct measurements of the 1630 cm^{-1} line of water (chosen in preference to the more intense lines around 3300 cm^{-1} because of its much smaller variation in the presence of electrolytes and with temperature) could be detected down to a concentration of 2.5%. Referencing the intensities of the two phases of the nitrate peak (in conjunction with measurements of the temperature of the system to correct for variations of the solubility of the nitrate) limits of

detection below 1% were achieved. Again, only two fibres were used to make these measurements (parallel 400 μm core fibres), so improvements in the collection optics and hence detection efficiencies are possible.

To reject the elastically scattered light from a sample, larger Raman spectrometers usually pre-filter the input light using a monochromator. Cooney and his coworkers[60] have described the use of holmium-doped sections of optical fibre as an effective means of filtering out the elastically scattered light from a Raman spectrum. By using the 488 nm line of an Argon laser, the elastically scattered light lay within an absorption band of the doped glass, and was removed, whereas the Raman light was not significantly affected. Clearly, however, one must avoid subsequent detection of undesirable fluorescent light from such a filter.

3.2 Gas-sensing

The most common method of optical gas sensing is spectral transmission analysis, which is employed in two principal regions of the optical spectrum. Absorption or emission lines in the shorter region, from 250 to 500 nm (the UV to visible-blue region) arise from electronic transitions. This is a very useful region of the spectrum for sensing the energetic changes that can occur within atoms or molecules of a large number of gaseous species.

The longer wavelength region, 1 to 8 μm, covers the near and mid-IR bands of the spectrum, a region where the vibrational absorptions of materials are more significant.

Typically a vibrational absorption 'line' will have a degree of fine structure superimposed on it, corresponding to the usually-lower-energy transitions associated with the rotational energy steps. (All these levels are of course quantised, into discrete allowed steps, according to the usual laws of quantum mechanics.)

Unfortunately, none of these transmission 'windows' corresponds to any region of the spectrum where gas absorption is high. Electronic absorptions usually occur in the UV and violet/blue regions of the spectrum, where fibre loss is very high. Most of the strong fundamental vibrational absorptions occur in the mid-IR at 2700 nm or longer, where silica is almost opaque. Thus, if it is desired to use conventional silica-based fibre, then the NIR absorption lines must be used. The use of long-path or multi-pass absorption cells is then necessary, to achieve even a moderate contrast in the measurement, and a well-designed opto-electronic system is necessary to reliably detect low levels of gases. As mentioned already, there are IR fibres based on more exotic materials (eg fluoride, silver halide or chalcogenide compounds) but, as stated, these fibres are expensive and fragile compared to silica fibres.

Examples of the sensing of gases by conventional optical methods are too numerous to list in full and can only be briefly mentioned here. A sample list of recent references in this area is given[61]-[71]. This list includes direct absorption methods[61],[64]-[69] and a photothermal method, where the resulting refractive index change is monitored by interferometry[62]. More recent papers use compact diode laser sources[63]-[68] or special long wavelength LEDs[64]. Because of the narrow absorption lines of many gases, the measurement contrast is generally much higher with narrow-band laser sources than with LEDs. A significant number[61],[63],[65],[66] have used the infra-red region of the spectrum, beyond the reach of silica-based fibre

systems, where gaseous absorption is generally greater. A number of more sophisticated methods have also been reported, eg correlation spectroscopy[69] and the use of frequency modulated laser sources which are rapidly swept through absorption lines[64].

In view of the extensive literature on gas spectrometry over many years, it is somewhat surprising that the first recognition of the potential for fibre-optic-remoted gas sensing should not be until 1979[71]. The researchers from a group at Tohoku University, Japan, pointed out the large number of (albeit rather weak) spectral absorption lines, which lie within the transmission window of a typical silica-based optical fibre. They pointed out the attraction of performing long-distance remote measurement over such links. In addition, the possibility of using liquid-core fibres (silica tubes, filled with carbon tetrachloride) for the mid-IR region was suggested, as such guides offer long wavelength transmission well beyond the cut-off of silica fibres, with a loss of only 56 dB/Km as far out as 3.39 μm (This is in spite of using a silica cladding, which contributes to the losses by evanescent-field absorption).

3.2.1 Nitrogen Dioxide Sensing

The first workers to demonstrate the technique in practice were from the same group at Tohoku University[72]. The gas chosen to demonstrate their method was nitrogen dioxide, a common impurity in vehicle exhaust gases, with a relatively long wavelength electronic absorption line at 496.5 nm. The method involved a single-channel, fibre-remoted spectrometer with two-wavelength referencing, one wavelength on the absorption line, the other displaced from the line of interest. The source, providing both the measurement line and a nearby reference line was a multi-line Argon ion laser. With a measurement-cell optical path length of 20 metres (using a multi-pass cell design to reduce size), and a response time constant of 1 second, a noise-limited sensitivity of approximately 17 ppm, was obtained. Measurements of nitrogen dioxide in exhaust gases from a motor cycle were taken, over a concentration range from 0 to 100 ppm.

3.2.2 Methane Gas Detection

The first demonstration of methane gas detection over optical fibre paths (figure 15)[73] was at the Electronics Research Laboratory of the Norwegian Institute of Technology, Trondheim. Their laboratory system used a broadband white light source, rotating-chopper and interference-filter arrangement, to sequentially interrogate the transmission of the sample cell, via a fibre optic cable link, and that of a more-direct (free-space), reference path. The measurement was broadband in nature, as the interference filter covered all the fine rotational line structure in the methane absorption band, (ie a 70 nm wide region, centred on 1.665 μm). The system effectively averaged the detected signal level over this wavelength range, giving rise to a very low contrast. Even on the peak of the individual lines, there is a relatively weak absorption at the low concentrations (usually <5% maximum) required to be measured. However, despite this, it was the first reported demonstration of methane detection over optical fibres, and had a respectable noise-limited sensitivity of 0.5% of the lower explosive limit (LEL) of methane (the LEL is approximately 5% methane in air). However, neither the long-term drift characteristics, nor the cross-sensitivity to other gases, were critically examined in this early paper.

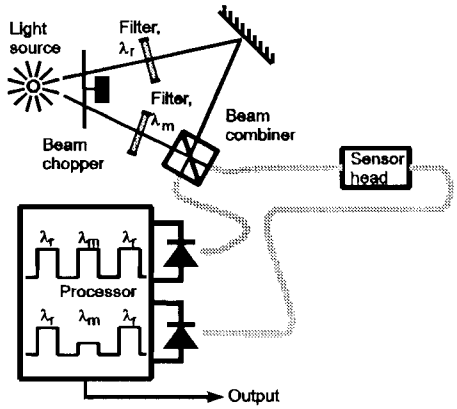

Figure 15 The remote methane sensing arrangement of Hordvick[73].

The first use of semiconductor LED sources for fibre remoted gas detection, in this case in conjunction with a fibre-remoted methanometer, was again reported by the Inaba group from Tohoku University[74]. A quaternary InGaAsP/InP device, having a laser structure, was operated, under lasing-threshold level, to provide an ELED source, having a centre wavelength of 1.61 μm and a 80 nm linewidth. The system was operated as a single beam absorption system (ie no reference path). The ELED was square-wave modulated and light was launched directly into the transmission fibre (figure 16). This fibre guided light over a 1 km path to the single-pass, sensing cell (0.5 metre long), and a similar fibre collected the transmitted light and guided it to a cooled Germanium detector, followed by a lock-in amplifier. The noise-limited resolution was equivalent to ≈ 0.07% of methane. In this simple laboratory demonstrator, however, there was no provision of a reference-path to guard against long term drift effects.

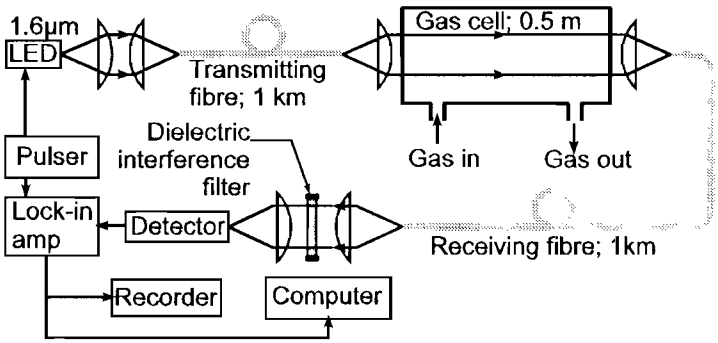

Figure 16 The remote methane sensing arrangement of Chan[74].

The first fibre-remoted methane detection scheme to be field tested was reported by Stueflotten[75] of A/S Elektrik Bureau, Norway. This system had much in common with the one just described, ie it used a compact chopped LED source and synchronous detection. However, steps were taken to enhance the long term stability of the system by using a dual-LED system, with one LED source centred on the absorption band and the other at an adjacent (non-absorbing) region of the spectrum (figure 17). These sources were alternately pulsed and the outputs combined into the input fibre using a passive coupler. On their return to the detector, after passage through a two-pass cell and the return fibre, the detected signal amplitudes from each source were electronically compared with a directly derived sample of the transmitted light signals. This allowed estimation of the degree of absorption which had taken place in the sample cell. The RMS-noise-limited sensitivity of the system, with a 1

second time constant, was ±1.5% LEL (equivalent to 0.075% methane). The system was reported to have been tested on a North Sea gas rig for 6 months. With this first prototype, it was indicated that problems in achieving the necessary long-term stability were experienced, due to temperature fluctuations in LEDs and wavelength-selective variations in the optical couplers, connectors and cables. It was claimed, however, that a new design had been developed which was expected to overcome these problems.

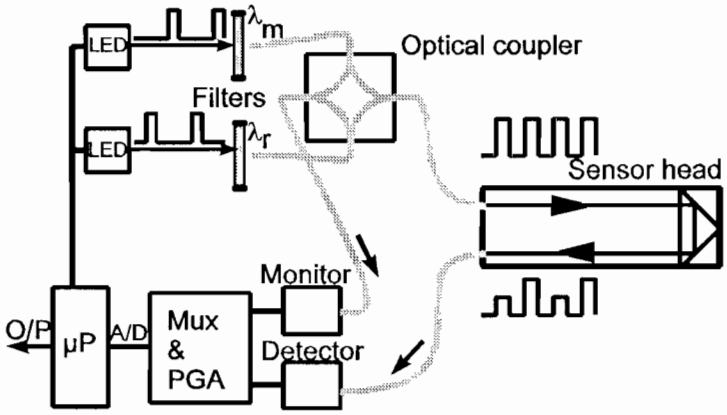

Figure 17 The arrangement of Steuflotten[24].

All the methane gas detection methods described above, were based on relatively broadband illumination of the gas, using either LED sources or interference filters having linewidths of the order of 20-100 nm. However, the absorption lines in the gas have natural linewidths much less than this and a far higher contrast can be achieved using narrow-band sources or filtered-detection systems. (The contrast in the measurement is an extremely important aspect, as a large fractional change helps to dominate problems of drift in signal level due to undesirable systematic effects). However, the use of a narrow-line laser as source can give rise to severe interferometric noise problems, due to speckle effects (ie the modal noise phenomena familiar in fibre optics communications systems). A method to help avoid this dilemma is to use a 'comb' filter, having a regularly-spaced series of narrow passbands, with wavelength spacing corresponding to that between the rotational absorption lines of the gas[76],[77], shown in figure 18a.

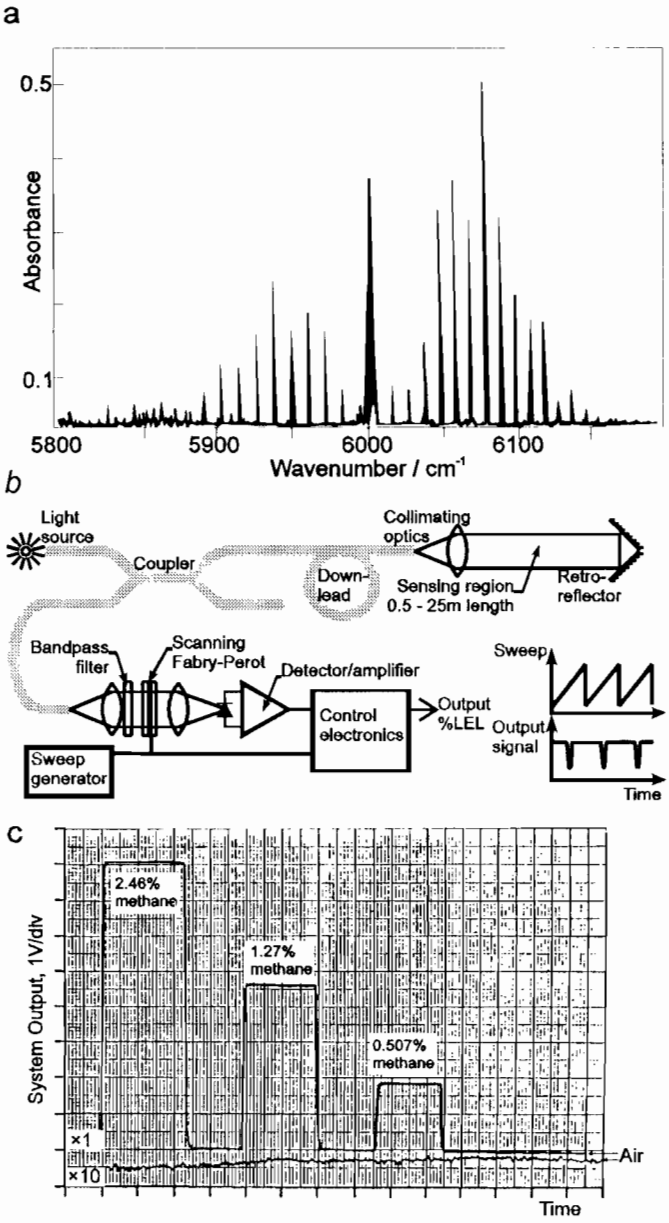

Figure 18 Methane detection using a scanned Fabry-Perot comb filter.

This increases the useful power that can be extracted from a broadband incandescent or LED source, as the combined effect of several absorption lines may be monitored and effectively decreases the coherence of the source. A suitable filter is a Fabry-Perot cavity, arranged to have the correct spacing to achieve the desired free spectral range. A further attraction of the approach is that the Fabry-Perot filter may be mechanically scanned to produce an 'AC' measurement, and allow referencing of the absorption signal, (ie the 'dip' in the signal when the filter coincides with the gas absorption lines) to the peak transmitted signal, (the flat peak level when the filtered bands lie between the gas absorption lines), figure 18b.

A further advantage is the strong selectivity of the method, because it tends to 'fingerprint' the gas absorption spectrum. The reported methods used typically 6 rotational lines for the

measurement, making the detected signal dependent on a matching of the Fabry Perot spacing to the characteristic line spacing, in addition to the absorption band location.

The response to methane gas, using a twin-pass (2 × 0.5 m) absorption cell, is shown in figure 18c[78]. With a 1 second measurement time constant, the noise-limited detection level of this method corresponded to ±0.003% RMS methane.

Two other narrow linewidth systems for the detection of methane have recently been reported. The first system, shown in figure 19, is based on the use of a twin-longitudinal mode, 1.33 μm GaInAsP (Fabry-Perot type) semiconductor laser diode[79]. The sensor also contains a scanning Fabry-Perot etalon, to alternately select one or other longitudinal mode of the laser. The laser was thermally tuned, until one mode corresponded with an absorption line of the methane gas. In spite of the very low absorption of the 1.33 μm band, the sensitivity of the results was good, mainly because of the high source power available in a very narrow line. (A noise limited sensitivity, of the order of ±0.05% methane, was reported in a 1 metre path length cell). The higher power available from the source should also enable multi-pass cells to be used, (although longer pathlengths can give rise to non-linearity in the response to the methane level).

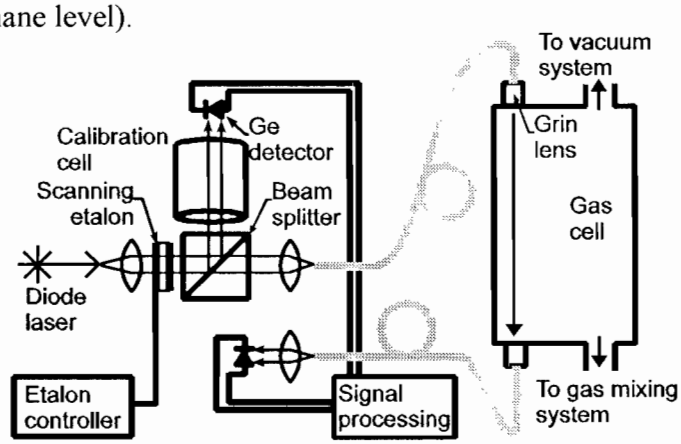

Figure 19 Gas sensor using diode laser source and etalon to select appropriate laser mode.

The second laser based method[80] used a Tm^{3+} fibre laser, tuned through a 1.685 μm methane line by stretching a wavelength-selective grating mirror. No particular laboratory problems with either of these methods were reported, although it might be anticipated that 'speckle' effects (ie the well-known modal noise phenomena) and, in the first case, laser mode-partition effects could be a possible source of error, particularly under more severe operational environments.

3.2.3 Hydrogen Gas Sensing

A novel system for hydrogen gas detection[81] is based on the dimensional expansion experienced by Palladium metal when it adsorbs hydrogen gas. This occurs by an interesting process, in which the gas is occluded at interstitial sites within the atomic lattice. The metal, in the form of thin wire, was bonded to one fibre arm of an all-fibre Michelson interferometer (see figure 20). The resulting linear dimensional change in the Palladium, which is proportional to the square root of the hydrogen partial pressure, is transferred to the fibre, resulting in changes in the output state of the interferometer. A hydrogen-partial-pressure resolution of ±2 Pascals was observed, equivalent to a hydrogen concentration of 20 ppm. A

problem with this initial laboratory system was that the attachment of the Palladium wire resulted in a differential expansion between the two dissimilar arms. Hence a temperature change of only 0.3 K could cause an effect equivalent to the 20 ppm detection limit. However, in a practical system, this source of error could be prevented, either by careful temperature control, or by expansion balancing of the arms of the fibre interferometer.

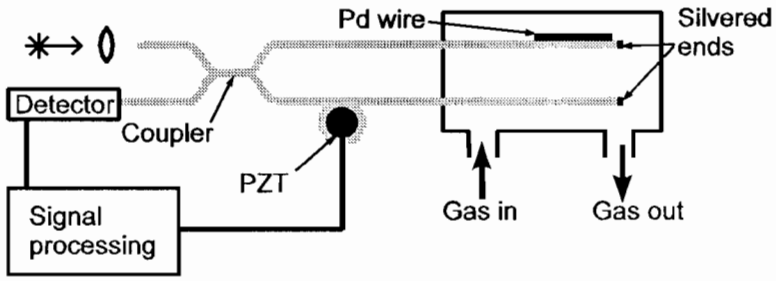

Figure 20 Experimental arrangement of H_2 sensor using occlusion in Pd[77]

3.2.4 Evanescent Wave Gas Sensing

All the above methods for gas sensing, with the exception of the palladium-based hydrogen sensor, have been of the extrinsic type (ie one using the fibre merely as a light guide, to and from the sensing region). It is now appropriate to describe intrinsic-type, sensors which use the evanescent field extending beyond the fibre core region to detect the gas in the vicinity of the fibre. The first method of this type was reported by Tanaka[82]. This paper reported an intrinsic sensor using a 50 μm/125 μm fibre, which was fused and stretched so that it tapered down to form a short, ultra-thin sensing region. Here the evanescent field could leak into the air surrounding the fibre. The sensor was used to detect the strong 3.39 μm methane absorption line. However, in this region the high losses in the silica fibre limited the total length of fibre to less than 3 metres. In addition, the noise-limited resolution limit was relatively poor, (of the order of 2% methane). Therefore, although of technical interest, it is less obvious how this technique might ultimately be applied, unless lower-loss infra red fibres were to be used. However, even when the fibre loss problem is solved there could be severe sensitivity to surface contamination.

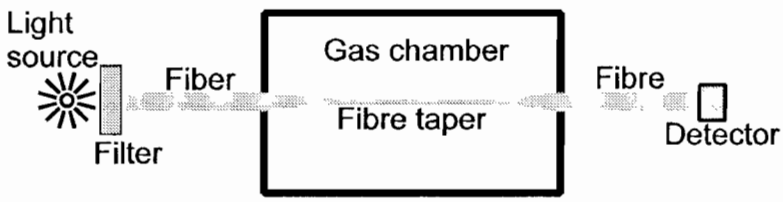

Figure 21 Measuring the absorption of a gas by fibre evanescent wave spectroscopy (FEWS).

An alternative to using tapers, which require sections of specially treated fibre, is to use non-cylindrical fibres which have the core region close to the outside surface. One example of this is the D-fibre, so called because of its D-shaped cross section, which brings the core close to the flat edge of the fibre[83]. Culshaw has used this method for gas detection[84]. The attraction is that, because of the constant cross section of the fibre, construction of a long sensing section is possible, with the further possibility of distributed sensing with an OTDR system. Jin has attempted to compensate for surface contamination[85] but this is likely to be difficult in real environments with variable temperature, non-uniform contamination and

bend sensitivity.

At the UV end of the spectrum, Potyrailo has used 1.8 m of coiled polysiloxane clad fibre to measure ozone absorption at 254 nm in concentrations between 0.06-0.35% by volume[86]. The polysiloxane cladding was permeable to gaseous ozone, with a typical diffusion time of the order of a minute, and showed no degradation over the two month period of the investigation. The limit of detection was calculated as 0.02%, and applications in water treatment, as well as ozone manufacturing, were foreseen.

3.2.5 Porous Glass Sensors

A final intrinsic sensor uses the ingenious idea of a vitreous gas-permeable fibre, constructed from a glass which has been designed to undergo phase separation. This glass composition permits chemical leaching out of an alkali-rich phase to leave a porous fibre structure of lower alkali content[87]. The microscopic dimensions of the pore structure (typically $\approx$ 1000 Å diameter), in such fibres, permits a strong optical interaction with the gaseous species and the method therefore shows promise for high sensitivity detection of many gases. The first demonstration of the porous fibre method was for the detection of water vapour, over a 0 to 50% relative humidity range. A response time of the order of 1 minute was achieved, but no long-term measurements were taken. Problems with the method could possibly occur due to surface adsorption, or due to the ingress of liquids into the pores by capillary action. As stated above, the great attraction of such intrinsic sensors are their potential for truly distributed sensors using OTDR. In order to be successful, the fibre attenuation and the degree of coupling between the incident optical field and the gas must be well characterised. In addition, good reversibility will normally be required. Although the early methods reported[82]-[90] show varying degrees of promise for such application, much more work must be done before they can be seriously used in systems. So far, none have yet been used in conjunction with OTDR systems, although reports of distributed measurements are expected to appear in the literature.

3.2.6 Photoacoustic Gas Sensing

Modulating or pulsing the photoacoustic excitation source causes a varying thermal expansion in the sample, which generates a series of acoustic waves propagating away from the optical path. These are detected using a microphone, which usually consists of a piezoelectric transducer made of a ceramic such as lead zirconate titanate (PZT), or a polymer such as poly [vinylidene difluoride] (PVDF). Condenser microphones have been used for gas-phase detection. However, as an interesting variation, an optical fibre sensor has been used with the eventual aim of enhancing sensitivity.

Optical detection of photoacoustic pressure waves

Two types of optical fibre interferometer for acoustic detection have been compared by Bregeut and co-workers[91]. A resonant azimuthal cell was used, with an optical microphone situated at a pressure antinode, and the optical excitation beam situated at a pressure node (chopped electrically at the frequency of cell resonance, 4 kHz). The microphone consisted of 2 m of monomode optical fibre coiled and bonded onto an aluminium plate.

Photoacoustic waves in the cell caused the microphone plate to be deflected, and the fibre to be periodically stretched, resulting in optical phase differences between the sensing beam and the reference beam. A Michelson interferometer and a Sagnac interferometer were compared, as shown in the schematic diagrams in figure 22.

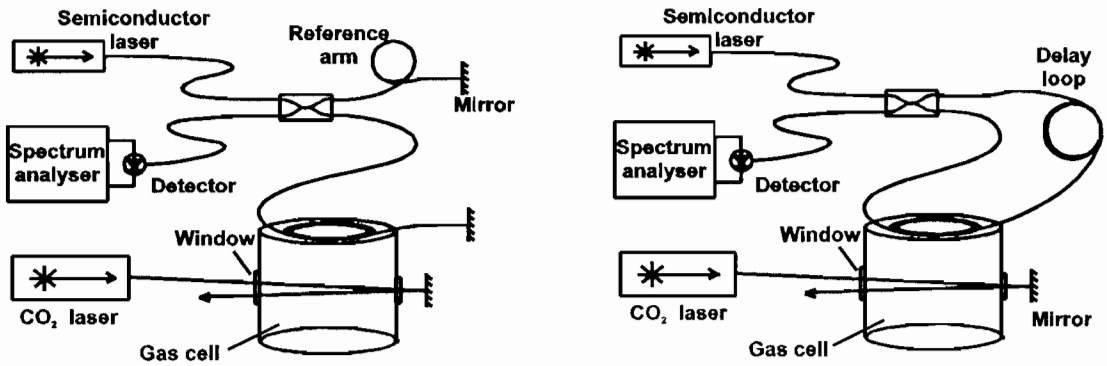

(a) Michelson interferomter **(b) Sagnac interferometer**

Figure 22. Interferometric detection of standing pressure waves in a resonant azimuthal photoacoustic cell. Picture modified from Bregeut[91].

The Sagnac interferometer had the advantages of greater stability (low-frequency environmental disturbances affect both interfering beams equally) and greater simplicity (there was no need to equalise the lengths of the sensing arm and the reference arm). Unfortunately, its performance was worse than an electrical microphone, which had a SNR seven times greater. The authors suggested that this may have been due to greater shielding of the electrical microphone from environmental acoustic noise. The sensitivity of the optical microphone could have been increased by lengthening the sensing fibre, and by better acoustic shielding, and therefore had promise of superior ultimate performance.

The work illustrates the advantage of using a resonant photoacoustic cell, to provide a mechanical 'amplification' of the photoacoustic pressure waves, by an amount depending on the quality factor Q of the resonance. Since the precise frequency of resonance will vary with temperature and pressure, active locking of the source modulation frequency to the resonant peak is usually needed to ensure large Q values, and so the system can become rather complex. It has been calculated that, without compensation, a change in temperature of 1 K, in a resonant cell with a Q of 500, can reduce the photoacoustic signal by a factor of 2[92].

3.2.7 Raman Spectroscopy for Gas Sensing

Raman scattering, which has excellent potential for general chemical analysis, has only recently been applied to optical fibre gas sensing[93] (figure 23). As described earlier in this chapter, the advantage of the method is its capability to interrogate energy levels normally associated with the mid and far-infrared, whilst using visible or near infra-red light in both the excitation and scattered beams. In addition, gases such as nitrogen, having no directly measurable IR absorption bands, can be measured, due to the different selection rules associated with Raman transitions. However, Raman scattered light from gas samples is

extremely weak. It was found necessary to use a photomultiplier, in photon counting mode, and to average for tens of seconds in order to detect the weak Raman light from a relatively concentrated gas sample[93], although little was done to maximise the signal by design of the Raman cell (eg. by arranging multiple reflections). An internally gold coated capillary cell has been used (as described for liquid phase analysis in section 2.7.3) by Dyer to demonstrate the possibility of using FT Raman instrumentation for the study of gases[94]. Using the capillary cell and 2.5 W excitation at 1064 nm the nitrogen in air could be seen at a 2:1 signal to noise ratio. Although the recorded spectra were of poor quality, due to the long wavelength excitation and poor detector responsivity, this technique is suited to remoting via optical fibres using shorter excitation wavelengths and dispersive instrumentation.

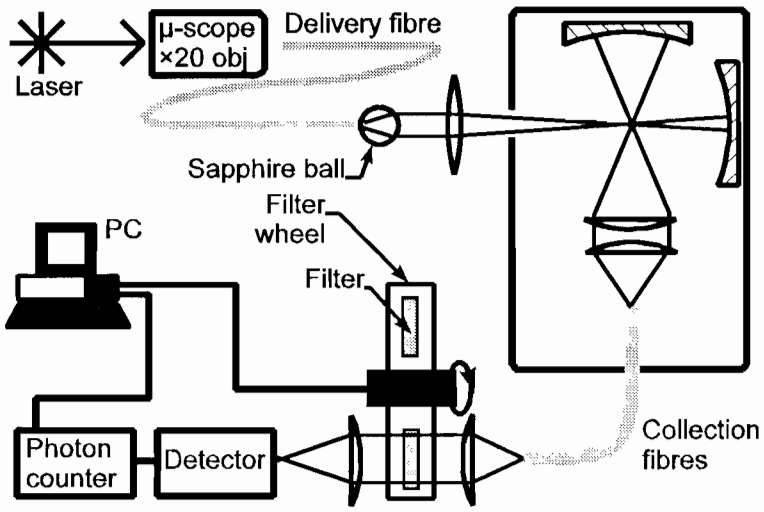

Figure 23 Gas sensing by Raman spectroscopy.

3.2.8 Correlation Spectroscopy for Gas Sensing

Early fibre-optic-based, gas-sensing methods measured transmission using broadband LED sources[73] and thus had poor selectivity. Other recent methods have used laser sources[95], but these can present problems due to the long coherence length; in particular modal noise effects in multimode fibre. Even when single-mode fibre is used to prevent this, effects such as Fabry-Perot etalons at connectors, and more complex interference patterns within the measurement cell and launch optics, can potentially cause severe practical limitations. Correlation spectroscopy[96-100] allows the use of a broadband source, yet still monitors the fine spectral features of the gas spectrum. It has the further advantage of employing all of the spectral information contained in the selected gas absorption band, rather than just a single line, thereby enhancing the cognitive nature of the technique.

The basic methods of real-time correlation spectrometry all involve modulation of the absorption spectrum of the reference gas sample relative to the gas to be measured. Modulation can be achieved directly by varying the absorption spectrum of the reference gas. In an early paper [99], progress with three modulation techniques was reviewed, each using the correlation spectroscopy method. These included Stark, pressure and phase modulation. The apparatus comprised two gas cells, through which light from a broadband source was passed sequentially, prior to detection. In the fibre-remoted version, light was conveyed to the cells via multimode optical fibre, and a bandpass filter was included before the detector in

order to attenuate light outside the absorption band of the relevant gas. The gas to be detected was directed into the measurement cell, whereas the reference cell was filled with a known concentration of the gas to be detected and then sealed.

Modulation of the absorption spectrum of either gas cell resulted in a change in the correlation between the spectrum of the measurement gas sample and that of the reference gas, thereby causing a variation in the transmission of the system, and hence in the detected signal. The absorption spectrum of the gas contained in the reference cell was modulated, either directly or indirectly, in order to produce the desired signal. The synchronously detected output signal then depended on the concentration of the correlating gas in the measurement cell.

Stark modulation of gases occurs only with polar molecules and results from the splitting (or, at atmospheric pressure the broadening) of individual absorption lines when a large electric field is applied. The pressure-modulation technique is more generally applicable. This involves periodically pressurizing the gas within the reference cell, causing a variation in both the strength and width of the absorption lines.

A third modulation approach is indirect and involves a redistribution of the optical spectrum of the light, as it passes from the measurement to the reference cell. Angle modulation of the light (using phase or frequency modulation) is a means of achieving this, which can be achieved using electro-optic (Pockel's cell) or acousto-optic (Bragg cell) respectively. Two more recent papers have considered improvements to correlation spectroscopy systems[101],[102].

4 Conclusions

The direct detection of chemicals using direct spectroscopy has been reviewed at some length. The treatment has been extremely detailed in view of the generic nature and industrial importance of many of the techniques. This is an area where many real commercial systems have already been developed (albeit many being simple extensions for laboratory spectrophotometers) and is likely to be an extremely important future area for fibres.

Acknowledgement

The authors would like to thank Dr Richard Harris for proof reading the final manuscript.

References

1. Thorne, AP; Spectrophysics (2nd Ed), Chapman and Hall Ltd (London), 1988.

2. Heitmann, W; Attenuation analysis of silica-based single-mode fibers, Journal of Optical Communications, 11, 122-129. 1990.

3. Senior, JM; Optical Fibre Communications Principles and Practice (2nd ed), Prentice Hall International (UK) Ltd, Hemel Hempstead. 1992.

4. Freeman, JE, Childers, AG, Steele, AW, Hieftje, GM; A fibre-optic based sensor for bioanalytical absorbance measurements, Analytical Chemistry, 56, 2246-2249. 1985.

5. Willis, HA, van der Maas, JH, Miller, RGJ [Eds]; Laboratory Methods in Vibrational Spectroscopy third edition, John Wiley and Sons, 1987.

6. Wolfbeis, OS [Ed]; Fiber Optic Chemical Sensors and Biosensors, Volume I, CRC Press. 1991.

7. Hecht, E; Optics [2nd ed], Addison-Wesley Publishing Company, Reading MA, 1987.

8. Rosencwaig, A; Photoacoustics and photoacoustic spectroscopy. Wiley, 1980, ISBN 0-89464-450-5

9. Pao, Yoh-Han (Ed); Optoacoustic spectroscopy and detection. Academic Press, 1977

10. Hess, P (Ed). Photoacoustic, photothermal and photochemical processes in gases. Springer-Verlag Topics in Current Physics - Volume 46, 1989.

11. Jackson, W B, Amer, N M, Boccara, A C and Fournier, D; Photothermal deflection spectroscopy and detection, Applied Optics, 20, 1223-1345. 1981.

12. Allen, CS, et al; Tunable laser excitation profile of surface enhanced Raman scattering from pyridine adsorbed on a copper electrode, Chemical Physics Letters, 75, 201. 1980.

13. Chang, RK, Furtak, TE [Eds]; Surface Enhanced Raman Scattering, Plenum Press, 1982.

14. Myrick, ML, Angel, SM; Elimination of background in fiber-optic Raman measurements, Applied Spectroscopy, 44, 565. 1990.

15. Ma, J, Ying-Sing, L; Fiber Raman background study and its application in setting up optical fiber Raman probes, Applied Optics, 35, 2527-2533. 1996.

16. Zhu, ZY, Yappert, MC; Determination of the effective depth for double-fiber fluorometric sensors, Applied Spectroscopy, 46, 919-924. 1992.

17. Plaza, P, Dao, NQ, Jouan, M, Fevrier, H, Saisse, H; Simulation et optimisation des capteurs á fibres optiques adjacents, Applied Optics, 25, 3448-3454. 1986.

18. Polytec X-dap product literature, Lambda Photometrics Ltd, Harpenden, UK.

19. Nave, SE, O'Rourke, PE, Malstrom, RA, Prather, WS; Fiber-optic Raman spectroscopy at the Savannah river site: uses and techniques, Process Control and Quality, 3, 43-48. 1992.

20. House of Hellma product literature, Hellma (England) Ltd, 23 Station Road, Westcliffe-on-Sea, Essex, SS0 7RA, UK.

21. Nave, SE, O'Rourke, PE, Toole, WR; Sampling probes enhance remote chemical analyses, Laser Focus World, 83-87. December 1995.

22. FCI Environmental, Inc; 1181 Grier Drive, Las Vegas, Nevada. (Geotechnical Instruments, in UK).

23. Kersey, AD, et al; Single-mode fibre Fourier transform spectrometer, Electronic Letters, 21, 463-464. 1985.

24. Jie, L, Brown, CW; Near-IR fiber optic probe for electrolytes in aqueous-solution, Analytical Chemistry, 65, 287-292. 1993.

25. O'Rourke, PE; Chemometrics/on-line measurements, JNMM, Journal of the Institute of Nuclear Materials Management, 18, 85-94. 1988.

26. Mittermayr, CR, Drouen, ACJH, Ott, M, Grasserbauer, M; Neural networks for library search of ultraviolet-spectra, Analytica Chimica Acta, 294, 227-45. 1994.

27. Long, JR, Vasilis, GG, Gemperline, PJ; Spectroscopic calibration and quantitation using artificial neural networks, Analytical Chemistry, 62, 1791-1797. 1990.

28. Zupan, J, Gasteiger, J; Neural networks: A new method for solving chemical problems or just a passing phase?, Analytica Chimica Acta, 248, 1-30. 1991.

29. Polani, ML; In Vivo Oximeter with Fast Dynamic Response, Review of Scientific Instruments, 22, 1050. 1962.

30. Proceedings of SPIE - The International Society for Optical Engineering, 1681, Optically Based Methods for Process Analysis, Somerset, NJ, USA, Mar 23-26, (Conf. code 17498). 1992.

31. Proceedings of SPIE - The International Society for Optical Engineering, 2365, Optical Sensing for Environmental and Process Monitoring, McLean, VA, USA, Nov 7-10, (Conf. code 22254). 1994.

32. Boisde, G, Blanc, F, Perez, J-J; Chemical measurements with optical fibers for process control, Talanta, 35, 75-82. 1988.

33. Coleman, JT, Eastham, JF, Sepaniak, MJ; Fiber-optic based sensor for bioanalytical absorbance measurements, Analytical Chemistry, 56, 2246-2249. 1984.

34. Krska, R, Kellner, R, Schiessl, U, Tacke, M, Katzir, A; Fiber optic sensor for chlorinated hydrocarbons in water based on infrared fibers and tunable diode lasers, Applied Physics Letters, 63, 1868-1870. 1993.

35. Simhony, S, Katzir, A; Fourier transform infrared spectra of organic compounds in solution and as thin layers obtained by using an attenuated total internal reflectance fiber-optic cell, Analytical Chemistry, 60, 1908-1910. 1988.

36. Krska, R, Rosenberg, E, Taga, K, Kellner, R; Polymer coated silver halide infrared fibers as sensing devices for chlorinated hydrocarbons in water, Applied Physics Letters, 61, 1778-1780. 1992.

37. Ertan-Lamontagne, MC, Lowry, SR, Seitz, WR, Tomellini, SA; Polymer-coated, tapered cylindrical ATR elements for sensitive detection of organic solutes in water, Applied Spectroscopy, 49, 1170-1173. 1995.

38. Degrendpre, MD, Burgess, LW; Fiber-optic FT-NIR evanescent field absorbance sensor, Applied Spectroscopy, 44, 273-279. 1990.

39. Bürck, J, Conzen, JP, Ache, HJ; A fiber optic evanescent field absorption sensor for monitoring organic contaminants in water, Fresenius Journal of Analytical Chemistry, 342, 394-400. 1992.

40. Bürck, J, Conzen, JP, Beckhaus, B, Ache, HJ; Fiber-optic evanescent wave sensor for in situ determination of non-polar organic compounds in water, Sensors and Actuators B, 18-19, 291-295. 1994.

41. Schwotzer, G, Latka, I, Lehmann, H, Willsch, R; Fiber optic evanescent field sensor for hydrocarbon monitoring in air and water applying UV absorption, OFS 11, Sapporo, Japan, 21-24 May 1996.

42. Sontag, H and Tam, AC; Optical detection of nanosecond acoustic pulses, IEE Transactions on Ultrasonics, Ferroelectrics and Frequency Control, vol UFFC-33, 500-506. 1986.

43. Hand, DP, Hodgson, P, Carolan, TA, Quan, KM, Mackenzie, HA and Jones, JDC; Detection of photoacoustic waves in liquids by fibre-optic interferometr, Optics Communications, 104, 1-6. 1993.

44. Hand, D P, Freeborn, S, Hodgson, P, Carolan, TA, Quan, KM, Mackenzie, HA and Jones, JDC; Optical fiber interferometry for photoacoustic spectroscopy in liquids, Optics Letters, 20, 213-215. 1995.

45. Tam, AC; Applications of photoacoustic sensing techniques, Reviews of Modern Physics, 58, R83-R121. 1986.

46. Tam, AC; Applications of photoacoustic sensing techniques, Review of Modern Physics, 58, 381-431. 1986.

47. Bohnert, B, Faubel, W, and Ache, HJ; Comparison of collinear and transverse photothermal deflection spectroscopy for trace analysis of pesticides in water, Fresenius Journal of Analytical Chemistry, 343, 513-517. 1992.

48. Vegetti, G, Martinelli, M, Balconi, L and Sigon, F; Photothermal detection of trace chemicals by fibre-optic interferometric probe. Springer series in optical sciences vol 69: Photoacoustic and photothermal phenomena III, Bićanić, D [Ed].

49. Klainer S, Hirschfeld T, Bowman HR, Milanovich FP, Perry D, Johnson D; A monitor for detecting nuclear waste leakage in a sub-surface repository Report, Livermore-Berkeley Laboratory 1981. 1981.

50. Chudyk, WA, Carrabba, MM, Kenny, JE; Remote detection of Ground water contaminants using far-ultraviolet laser induced fluorescence, Analytical Chemistry, 57, 1237. 1985.

51. Berlman, IB; Handbook of Fluorescent Spectra of Aromatic Molecules, 2nd Ed, Academic Press, New York, 1974.

52. Bublitz, J, Dickenhausen, M, Gräz, M, Todt, S, Schade, W; Fiber-optic laser-induced fluorescence probe for the detection of environmental pollutants, Applied Optics, 34, 3223. 1995.

53. Panne, U, and Neissner, R; A fibre-optical sensor for polynuclear aromatic hydrocarbons, based on multidimensional fluorescence, Sensors and Actuators, B, 13-14, 288. 1993.

54. Hillrichs, G, Karlitschek, P, Neu, W; Fiber optic aspects of UV laser spectroscopic in situ detection of water pollutants, SPIE Proceedings Vol. 2293 Chemical, Biochemical, and Environmental Fiber Sensors VI, 07/24 - 07/29/94, San Diego, CA, USA .

55. Dmitriev, VG, Gurzadyn, GG, Nikogosyan, DN; Handbook of Nonlinear Optical Crystals, Springer, 1991.

56. Demas, JN and Keller, RA; Enhancement of luminescence and Raman spectroscopy by phase-resolved background suppression, Analytical Chemistry, 57, 539. 1985.

57. Mackenzie, SJ, Dakin, JP; Internally Teflon-AF coated capillary cell for optical fibre remote spectroscopy, CLEO/Europe-EQEC, Hamburg 8-13 September, 1996.

58. Chike, KE et al; Raman and near-infrared studies of an epoxy resin, Applied Spectroscopy, 47, 1631. 1993.

59. Lombardi, DR, Mann, CK, Vickers, TJ; Determination of water in slurries by fiber-optic Raman spectroscopy, Applied Spectroscopy, 49, 220-224. 1995.

60. Cooney, TF et al; Rare-earth doped glass fiber for background rejection in remote fiber-optic Raman probes: Theory and analysis of Holmium-bearing glass, Applied Spectroscopy, 47, 1683. 1993.

61. Edwards, DK; Absorption by infrared bands of carbon dioxide at elevated pressures and temperatures, Journal of the Optical Society of America, 50, 617-626. 1960.

62. Davis, CC, Petuchowski, SJ, Phase fluctuation optical heterodyne spectroscopy of gases, Applied Optics, 20, 2539-2554. 1981.

63. Koga, R, Kosaka, M, Sano, H; Field methane tracking with a portable and real-time open-gas monitor, based on a cw-driven Pb-salt laser, Optics and Laser Technology, 17, 139-144. 1985.

64. Aagard, RT, et al; Development of a selective natural gas detector, Proceedings of International Gas Research Conference, Toronto, September, 1986.

65. Forrest, GT; Simple diode laser spectroscopy from 6 to 10 microns, Spectrochimica Acta 42a, 281-284. 1986.

66. Silver, J, Stanton, AC; Airborne measurements of humidity using a single-mode Pb-salt diode laser, Applied. Optics, 26, 2558-2566. 1987.

67. Milton, MJ, Woods, PT; Pulse averaging methods for a laser remote monitoring system using atmospheric backscatter, Applied Optics, 26, 2598-2603. 1987

68. Cassidy, DT; Trace Gas detection using 1.3 μm InGaAsP diode laser transmitter modules, Applied Optics, 27, 6120-6140. 1988.

69. Margolis, JS, McCleese, DJ, Martonchik, JV; Remote Detection of Gases by Gas Correlation Spectro-radiometry, Optical and Radar Remote Sensing, edited by Killinger, DK, and Mooradian, A; Springer Series on Optical Sciences, 39, 114-117, 1983.

70. Wang, L, Rires, H, Carlisle, CB, Gallagher, TF; Comparison of approaches to modulation spectroscopy with GaAlAs semiconductor lasers: water vapour, Applied Optics, 27, 2071-2077. 1988.

71. Inaba, H, et al; Optical fiber network system for air-pollution monitoring over a wide area by optical absorption method, Electronics Letters. 15, 749-751. 1979.

72. Kobayasi, T, Hirama, M, Inaba, H; Remote monitoring of nitrogen dioxide molecules by differential absorption using optical fibre link, Applied Optics, 20, 3279-3280. 1981.

73. Hordvik, A, Berg, A, Thingbo, D; A fiber optic gas detection system, Proceedings of 9th European Conference on Optical Communications, Geneva, Switzerland, 1983, p 317.

74. Chan, K, Ito, H, Inaba, H; An Optical fiber-based gas sensor for remote absorption measurements of low-level methane gas in the near-infrared region, Journal of Lightwave Technology 2, 234-237. 1984.

75. Stueflotten, S, et al; An infrared fibre optic gas detection system, Proceedings of OFS'84 International Conference, Stuttgart, 87-90. 1984.

76. Dakin, JP, Wade, CA, Pinchbeck, D, Wykes, JS; A novel optical fibre methane sensor, Proceedings of SPIE International Conference on Fiber Optics '87, London, 734, 33. 1987.

77. Dakin, JP, Croydon, WF, Hedges, NK; A fiber optic methane sensor having improved performance, Proceedings of SPIE International Conference on Fiber Optics '88, London, 949, 30. 1988.

78. Dakin, JP, Croydon, WF; Applications of fiber optics in gas sensing, Review at ECOC/LAN, Amsterdam, June 1988. (No full written version of this review paper was given in proceedings - results described in the current text were shown during the presentation). 1988.

79. Mohebati, A, King, TA; Remote detection of gases by diode laser spectroscopy, Journal of Modern Optics, 35, 310-324. 1988.

80. Barnes, WL, Dakin, JP, Edwards, HO, Reekie, L, Townsend, JE, Murray, S, Pin, D; Tunable fibre laser sources for methane detection at 1.68 μm, Proceedings of SPIE International Conference on Chemical, Biochemical and Environmental Sensors IV, Boston 8-11 September 1992, p 1796.

81. Farahi, F, et al; Fibre Optic interferometric hydrogen sensor, Proceedings of OFS'86 International Conference, Tokyo, 127-130. 1986.

82. Tanaka et al; Fiber-optic evanescent wave gas spectroscopy, Proceedings of OFS'86 International Conference, Tokyo, Post Deadline Paper 2-1. 1986.

83. Stewart, G, Culshaw, B; Optical wave-guide modelling and design for evanescent field chemical sensors, Optical and Quantum Electronics, 26, S249-S259. 1994.

84. Muhammad, FA, Stewart, G, Jin, W; Sensitivity enhancement of D-fiber methane gas sensor using high index overlay, IEE Proceedings-Journal of Optoelectronics, 140, 115-118. 1993.

85. Jin, W, Stewart, G, Wilkinson, M, Culshaw, B, Muhammad, F, Murray, S, Norris, JOW; Compensation for surface contamination in a D-fiber evanescent-wave methane sensor, Journal of Lightwave Technology, 13, 1177-1183. 1995.

86. Potyrailo, RA, Hobbs, SE, Hieftje, GM; Near ultraviolet evanescent-wave determination of ozone with fiber optics, prepared for submission to Analytical Chemistry. 1996.

87. Shahriari, MR, Sigel Jnr, GH, Zhou, Q; Porous Fiber optics for a high sensitivity humidity sensor, Proceedings of OFS'88 International Conference, New Orleans, 373-381. 1988.

88. Surgi, MR; The design and evaluation of a reversible fiber optic sensor for determination of oxygen, Proceedings of OFS'88, New Orleans, 349-352. 1988.

89. Beyler, LL, Ferrara, JA, MacChesney, JB; A plastic-clad silica fiber chemical sensor for ammonia, Proceedings of OFS'88 International Conference, New Orleans, 369-372. 1988.

90. Liebermann, RA, Beyler, LL, Cohen, LG; Distributed fluorescence oxygen sensor, Proceedings of OFS'88 International Conference, New Orleans, 346-348. 1988.

91. Breguet, J, Pellaux, JP and Gisin, N; Photoacoustic detection of trace gases with an optical microphone, Sensors and Actuators A, 48, 29-35. 1995.

92. Tilden, SB, Denton, MB; Theory and evaluation of a windowless non-resonant optoacoustic cell, Applied Spectroscopy, 39, 1022-1029. 1985.

93. Samson, PJ; Fibre optic gas sensing using Raman spectrometry, Proceedings of the 14th Australian Conference on Optical Fiber Technology, Brisbane, Dec 1989, 145-148. 1989.

94. Dyer, CD, Hendra, PJ; Near-infrared Fourier transform Raman spectroscopy of gases, Analyst, 117, 1393-1399. 1992.

95. Kobayasi T, Hirana M, Inaba H; Remote monitoring of NO_2 molecules by differential absorption using optical fibre link. Applied Optics, 20, 3279. 1981.

96. Goody, R; Cross-correlating spectrometer, Journal of the Optical Society of America, 58, 900. 1986.

97. Taylor, FW, Houghton, JT, Peskett, GD, Rogers, CD, Williamson, EJ; Radiometer for remote sounding of the upper atmosphere, Applied Optics, 1, 135. 1972.

98. Edwards, HO, Dakin, JP; A novel optical fibre gas sensor employing pressure-modulation spectrometry, Proceedings of 7th Optical Sensors Conference, Sydney, Australia, 55. 1990.

99. Dakin, JP, Edwards, HO; Gas sensors using correlation spectroscopy, compatible with fibre optic operation, Sensors and Actuators B, 11, 9-19. 1993.

100. Dakin, JP, Edwards, HO; Progress in fiber-remoted gas correlation spectrometry, Optical Engineering, 31, 1616-1620. 1992.

101. Dakin, JP, Edwards, HO, Weigl, BH; Progress with optical gas sensors using correlation spectroscopy, Sensors and Actuators B, B29, 87-93. 1995.

102. Dakin, JP; Latest developments in gas sensing using correlation spectroscopy, Proceedings of SPIE, Optics of Environmental and Public Saftey, Munich, 19-23 June 1995, vol 2508.